4

Pulsatile Flow in a Rigid Tube

4.1 Introduction

Flow in a tube in which the driving pressure varies in time is governed by Eq.3.2.9, namely,

$$\rho\frac{\partial u}{\partial t} + \quad \frac{\partial p}{\partial x} = \mu\left(\frac{\partial^2 u}{\partial r^2} + \frac{1}{r}\frac{\partial u}{\partial r}\right)$$

Providing that all the simplifying assumptions on which the equation is based are still valid, the equation provides a forum for a solution in which the pressure p is a function of x and t while the velocity u is a function of r and t. Before obtaining this solution, it is important to reiterate the assumptions on which the equation is based, because these assumptions define the idealized features of the flow that the solution represents.

For the purpose of discussion we consider a specific case in which the driving pressure is oscillatory in time, varying as a trigonometric sine or cosine function. As the pressure rises to its peak, the flow increases gradually in response, and as the pressure falls, the flow follows again. If the change in pressure is very slow, the corresponding change in flow will be almost in phase with it, but if the change in pressure is rapid, the flow will lag behind because of the inertia of the fluid. Because of this lag, the peak that the flow reaches in each cycle will be somewhat short of what it would be in steady Poiseuille flow under a constant driving pressure equal to the peak of the oscillatory pressure.

This loss in peak flow is higher at higher frequency of oscillation of the driving pressure, to the point that at very high frequency the fluid barely

moves at all. Only at the other extreme, at very *low* frequency, will the flow rise and fall in phase with the pressure and reach a peak commensurate with the peak pressure at each cycle. In fact at very low frequency the pressure and flow are *instantaneously* what they would be in steady Poiseuille flow. That is, the Poiseuille relation between pressure and flow (Eq.3.4.3) is satisfied at every instant in the oscillatory cycle as they both change during the cycle. Not only the flow rate but the velocity profile at each instant will also be the same as it would be in steady Poiseuille flow under a constant driving pressure equal to the value of the oscillatory pressure at that instant in the oscillatory cycle, at *low* frequency. At *high* frequency the velocity profile fails to reach the full form that it would have reached in Poiseuille flow under the same driving pressure.

The assumptions under which this oscillatory flow takes place are essentially the same as those in steady Poiseuille flow. The cross section of the tube must be circular and axial symmetry must prevail to the effect that velocity and derivatives in the θ direction are zero. Also, the tube must be sufficiently long for the flow field to be fully developed and independent of x, and we saw in Section 3.2 that this requires that the tube be *rigid*. The consequences of these restrictions are far more significant in pulsatile flow than in steady Poiseuille flow.

In order to satisfy these restrictions in pulsatile flow, fluid at different axial positions along the tube must respond *in unison* to the changing pressure, to the effect that the velocity profile is *instantaneously* the same at all axial positions along the tube. As the pressure changes, the velocity profile changes in response, simultaneously at all axial positions along the tube. It is as if the fluid is moving in bulk.

While this feature of the flow is fairly artificial and somewhat "unphysical," it provides an important foundation for the understanding of more realistic forms of pulsatile flow. In fact the classical solution that we present in this chapter and that has provided the basic understanding of pulsatile flow is based on this model of the flow.

To make the model more realistic, the tube must be allowed to be nonrigid. As the pressure changes in a nonrigid tube, the change acts only locally at first because it is able to stretch the tube at that location (Fig.5.1.1). Later the stretched section of the tube recoils and pushes the change in pressure further down the tube. This produces a *wave*, which travels down the tube [1]. *In the case of a rigid tube there is no wave motion.* The flow in a rigid tube rises and falls simultaneously at all axial positions along the tube.

In the presence of wave motion the axial velocity u is a function of not only r and t but also of x, and the radial velocity v is no longer zero, thus Eq.3.2.9 ceases to be valid. More important, the presence of wave motion entails the possibility of *wave reflections*, which introduce further complications in the analysis of the flow. These complications are considered in subsequent chapters. In this chapter we present the classical solution of

Eq.3.2.9, which is bas
tube.

4.2 Oscillatory Flow Equations

The pumping action of the heart produces a pressure difference across the arterial tree, which changes rhythmically with that action. It is a characteristic of this driving force that it consists of a constant part that does not vary in time and that produces a steady flow forward as in Poiseuille flow, plus an oscillatory part that moves the fluid only back and forth and that produces zero net flow over each cycle. We shall use the terms "steady" and "oscillatory" to refer to these two components of the flow, respectively, and the term "pulsatile" to refer to the combination of the two.

An important feature of Eq.3.2.9 is that it is *linear* in both the pressure $p(x,t)$ and velocity $u(r,t)$. As a result of this feature the equation can deal with the steady and oscillatory parts of the flow entirely separately and independently of each other. This is a useful breakdown of the problem, because the steady part of the flow has already been dealt with in Chapter 3.

The oscillatory part of the problem can be isolated and dealt with separately, which we do in the present chapter. This part of the problem is mathematically more complicated than the steady-flow part, and in the midst of the analysis to follow it may seem pointless to consider it since it only moves fluid back and forth with no net flow. It is therefore helpful to remember that the reason for which the ocillatory part is dealt with in such great detail is that it represents an important part of the composite pulsatile flow that we are interested in, and it carries with it most of the seminal features of the composite flow.

If the steady and oscillatory parts of the pressure and velocity are identified by subscripts "s" and "ϕ," respectively, then to isolate the oscillatory flow problem we write

$$\begin{aligned} p(x,t) &= p_s(x) + p_\phi(x,t) \\ u(r,t) &= u_s(r) + u_\phi(r,t) \end{aligned} \tag{4.2.1}$$

Substituting these into Eq.3.2.9, we obtain

$$\begin{aligned} &\left\{ \frac{dp_s}{dx} - \mu\left(\frac{d^2u_s}{dr^2} + \frac{1}{r}\frac{du_s}{dr} \right) \right\} \\ + &\left\{ \rho\frac{\partial u_\phi}{\partial t} + \frac{\partial p_\phi}{\partial x} - \mu\left(\frac{\partial^2 u_\phi}{\partial r^2} + \frac{1}{r}\frac{\partial u_\phi}{\partial r} \right) \right\} = 0 \end{aligned} \tag{4.2.2}$$

where terms have been grouped into those that do not depend on time t (first group) and those that do (second group). Because of that difference between them, each group must equal zero separately.

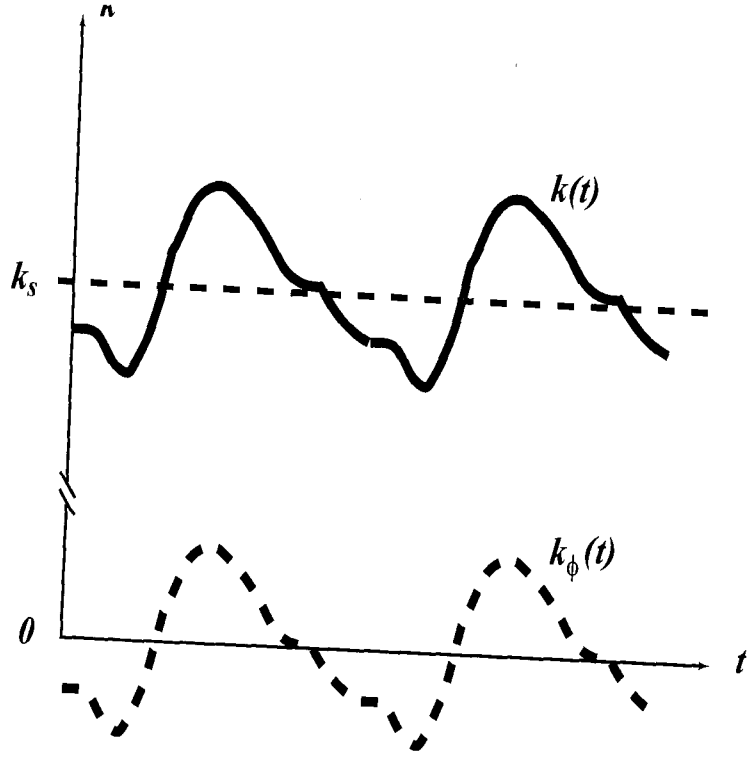

FIGURE 4.2.1. Pulsatile pressure gradient $k(t)$ consists of a constant part k_s and a purely oscillatory part $k_\phi(t)$.

The first equality then leads to Eq.3.3.2 for steady flow, which has already been dealt with, and the second leads to a governing equation for the oscillatory part of the flow, namely,

$$\rho\frac{\partial u_\phi}{\partial t}+\frac{\partial p_\phi}{\partial x}-\mu\left(\frac{\partial^2 u_\phi}{\partial r^2}+\frac{1}{r}\frac{\partial u_\phi}{\partial r}\right)=0 \tag{4.2.3}$$

Equations 3.3.2 and 4.2.3 are entirely independent of each other in the sense that the first can be solved for u_s, which has already been done, and the second can be solved separately for u_ϕ, which we do in what follows.

Furthermore, because of the independence of the steady- and oscillatory-flow equations, and for reasons similar to those in steady flow, the relation between pressure *gradients*, from Eq.4.2.1, is

$$k(t)=k_s+k_\phi(t) \tag{4.2.4}$$

where

$$k(t)=\frac{\partial p}{\partial x}$$

$$k_s=\frac{dp_s}{dx}$$

$$k_\phi(t)=\frac{\partial p_\phi}{\partial x} \tag{4.2.5}$$

Thus $k(t)$ is the "total" pressure gradient in pulsatile flow, k_s is its steady part, and k_ϕ is its purely oscillatory part, as illustrated in Fig.4.2.1

In steady Poiseuille flow the pressure gradient term in the governing equation (Eq.3.3.2) is found to be constant, independent of x, essentially because all other terms in the equation are functions of r only, while the pressure is a function of x only. Similarly, in oscillatory flow the pressure gradient term in the governing equation (Eq.4.2.3) is independent of x, for the same reasons, but here it can be a function of time t.

As k_s in steady Poiseuille flow, k_ϕ here is a measure of the pressure difference $\triangle p_\phi$ between the two ends of the tube, which in the present case is a function of time. In analogy with Eq.3.4.9, here

$$\triangle p_\phi=p_\phi(l,t)-p_\phi(0,t)=k_\phi(t)l \tag{4.2.6}$$

where l is the length of the tube and $p_\phi(x,t)$ is the pressure at axial position x along the tube and at time t. The governing equation for oscillatory flow, from Eq.4.2.3, is then of the form

$$\mu\left(\frac{\partial^2 u_\phi}{\partial r^2}+\frac{1}{r}\frac{\partial u_\phi}{\partial r}\right)-\rho\frac{\partial u_\phi}{\partial t}=k_\phi(t) \tag{4.2.7}$$

4.3 Fourier Analysis

For the oscillatory problem to be physically determined, the way in which the driving pressure varies in time must be given. That is, in order to solve Eq.4.2.7 for $u_\phi(r,t)$, $k_\phi(t)$ must be specified. We are interested in a solution for which $k_\phi(t)$ is an oscillatory function of time, to model the oscillatory pressure produced by the heart discussed in the previous section. However, the oscillatory pressure produced by the heart is not a simple function of time for which a direct solution of Eq.4.2.7 is possible.

One way of dealing with this difficulty is to specify $k_\phi(t)$ *numerically* as a function of time, then Eq.4.2.7 would have to be solved numerically. Another way is offered by the fact that any periodic function can be expressed as a sum of sine and cosine functions, known as a *Fourier series.*

Briefly, a function $f(t)$ is periodic if

$$f(t+T)=f(t) \tag{4.3.1}$$

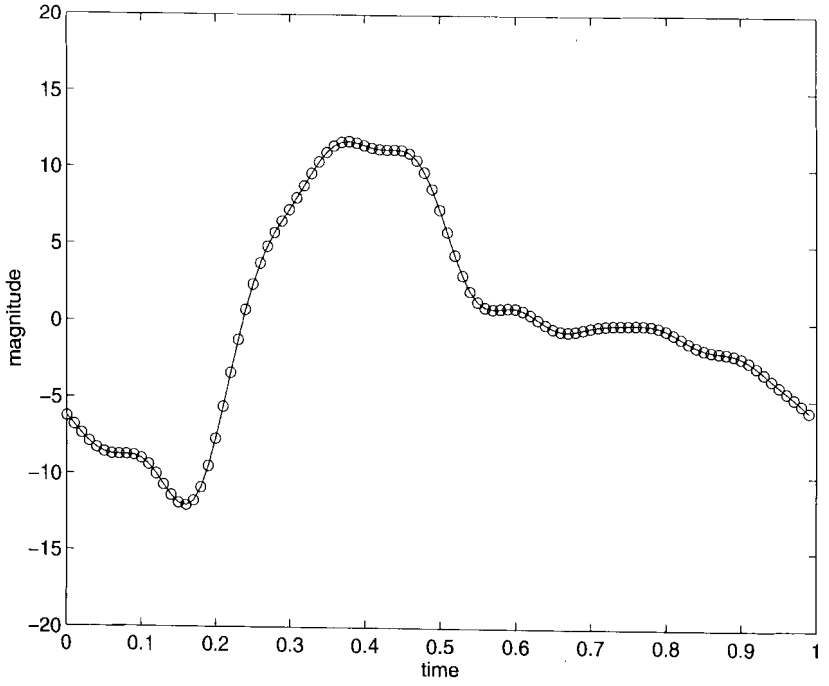

FIGURE 4.3.1. Typical composite pressure waveform produced by the heart. Only the oscillatory part of the wave is shown, the constant part has been removed.

where T is the "period" of the function. A periodic function can be represented by the Fourier series [2]

$$f(t) = \sum_{0}^{\infty} A_n \cos\left(\frac{2n\pi t}{T}\right) + \sum_{1}^{\infty} B_n \sin\left(\frac{2n\pi t}{T}\right)$$

$$= A_0 + A_1 \cos\left(\frac{2\pi t}{T}\right) + A_2 \cos\left(\frac{4\pi t}{T}\right) + \ldots$$

$$+ B_1 \sin\left(\frac{2\pi t}{T}\right) + B_2 \sin\left(\frac{4\pi t}{T}\right) + \ldots \qquad (4.3.2)$$

where the A's and the B's are constants that are determined by the specific characteristics of $f(t)$ and are given by

$$A_0 = \frac{1}{2\pi}\int_0^{2\pi} f(t)dt$$

$$A_n = \frac{1}{\pi}\int_0^{2\pi} f(t)\cos\left(\frac{2n\pi t}{T}\right)dt$$

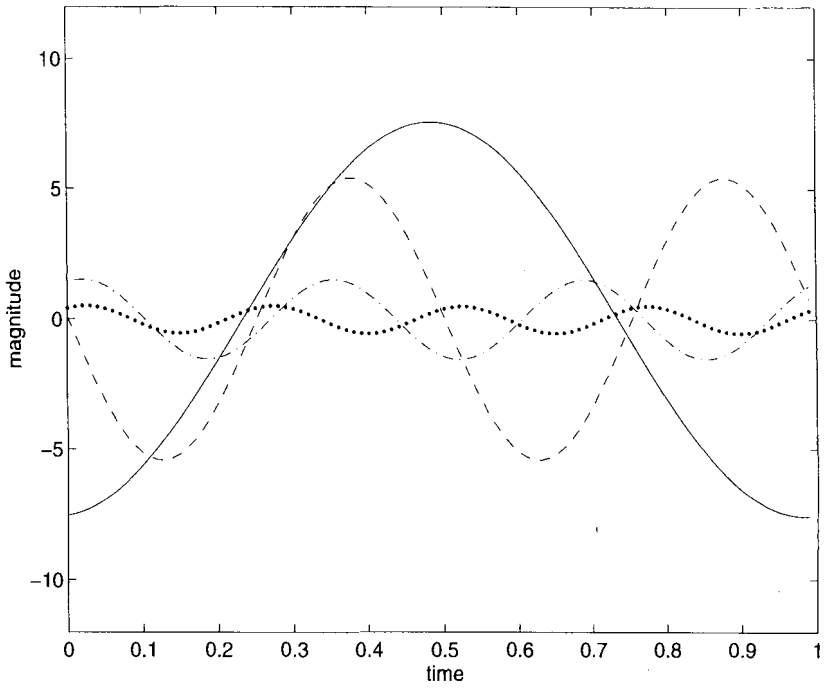

FIGURE 4.3.2. The first four harmonics of the composite waveform shown in Fig.4.3.1. The first harmonic (solid line) has the same frequency as the composite wave, then each subsequent harmonic is a multiple of the first. Note the diminishing amplitude of higher harmonics.

$$B_n = \frac{1}{\pi}\int_0^{2\pi} f(t)\sin\left(\frac{2n\pi t}{T}\right)dt \qquad (4.3.3)$$

Thus any arbitrary form of $k_\phi(t)$ in Eq.4.2.7, so long as it is a *periodic* function, can be expressed as a Fourier series consisting of a sum of sines and cosines known as its "harmonics" [2]. It will be noted from Eq.4.3.2 that the nature of these harmonics is such that the first harmonic has the same frequency as the original waveform, the second has double that frequency, and so on. Thus the original composite waveform can be decomposed into a "recipe" of sine and cosine waves of increasing frequency and, as we shall see, diminishing amplitude. This makes the method of great practical use because only a relatively small number of harmonics (10 or less) are usually required to represent the composite wave with reasonable accuracy. An example of an oscillatory waveform produced by the heart is shown in Fig.4.3.1, with its first four harmonics shown in Fig.4.3.2.

The advantage of a solution based on this approach is twofold. First, since Eq.4.2.7 is *linear* in u_ϕ, a sum of sine and cosine terms on the right can be taken only one term at a time, then adding the results. Thus the equation, in effect, need be solved with only one sine or cosine term on the

right. Second, Eq.4.2.7 has an exact analytical solution when $k_\phi(t)$ is a sine or cosine function, which has many advantages over a numerical solution.

Added to these advantages is the fact that in most practical cases the infinite Fourier series in Eq.4.3.2 can be approximated by a sum of only 10 or so terms. And the process of decomposition of the solution and re-synthesis of the results have been automated by many computer programs, which handle all the tedious details [3]. Thus the classical solution that we present in what follows, which is highly idealized in that it is based on a driving pressure which varies as a sine or cosine function, is in fact an essential element of a more realistic solution in which the pressure varies as a more general oscillatory function.

4.4 Complex Pressure Gradient and Bessel Equation

Solution of Eq.4.2.7 with the oscillatory pressure gradient being taken as a sine or cosine function is much simplified analytically if, instead of using one or the other, their complex combination in exponential form is used, that is, taking

$$k_\phi(t) = k_s e^{i\omega t} = k_s(\cos\omega t + i\sin\omega t) \tag{4.4.1}$$

where $i = \sqrt{-1}$. Because Eq.4.2.7 is linear, a solution with this choice of k_ϕ will actually consist of the sum of *two* solutions, one for which $k_\phi(t) = k_s\cos\omega t$ and another for which $k_\phi(t) = k_s\sin\omega t$. The first is obtained by taking the real part of the solution and the second by taking the imaginary part. The combined solution is complex because of this choice of $k_\phi(t)$.

For the purpose of comparison with steady Poiseuille flow in which the driving pressure gradient is constant, k_s, the amplitude of the oscillatory pressure gradient in Eq.4.4.1 is taken as k_s. In this way the peak value of the oscillatory flow rate and peak form of the oscillatory velocity profile can be compared with the flow rate and velocity profile in steady Poiseuille flow with constant pressure gradient k_s.

The governing equation for oscillatory flow with this choice of pressure gradient is then, using Eqs.4.4.1 and 4.2.7,

$$\frac{\partial^2 u_\phi}{\partial r^2} + \frac{1}{r}\frac{\partial u_\phi}{\partial r} - \frac{\rho}{\mu}\frac{\partial u_\phi}{\partial t} = \frac{k_s}{\mu}e^{i\omega t} \tag{4.4.2}$$

The form of the equation admits a solution by separation of variables, that is, by a decomposition of $u_\phi(r,t)$ into one part that depends on r only and one on t only. Furthermore, the form of the equation and the exponential form of the function of time on the right-hand side together dictate that the part of u_ϕ which depends on t must have the same exponential form as that on the right-hand side. The separation of variables thus arrived at is

$$u_\phi(r,t) = U_\phi(r)e^{i\omega t} \tag{4.4.3}$$

Upon substitution in Eq.4.4.2, the factor $e^{i\omega t}$ cancels throughout, leaving an ordinary differential equation for $U_\phi(r)$ only, namely,

$$\frac{d^2U_\phi}{dr^2} + \frac{1}{r}\frac{dU_\phi}{dr} - \frac{i\Omega^2}{a^2}U_\phi = \frac{k_s}{\mu} \tag{4.4.4}$$

where a is the tube radius and Ω is an important nondimensional parameter, given by

$$\Omega = \sqrt{\frac{\rho\omega}{\mu}}a \tag{4.4.5}$$

We shall see later that the value of Ω has a significant effect on the form of the solution.

It is clear that Eq.4.4.4, being an *ordinary* differential equation, is considerably simpler than Eq.4.4.2. In fact Eq.4.4.4 is a form of Bessel equation, which has a standard solution as we see in the next section [4,5].

It is important to note that this simplification of the problem has been achieved primarily by the simple choice of $k_\phi(t)$ in Eq.4.4.1. This simplified form of the problem is fundamental, however, and is in fact a prerequisite for dealing with more complicated forms of $k_\phi(t)$ as discussed in the previous section. It is also important to note that while the pressure gradient $k_\phi(t)$ in Eq.4.4.1 and the velocity $u_\phi(r,t)$ in Eq.4.4.3 appear to have the same oscillatory form in the time variable t, this does not mean that the pressure gradient and velocity are actually in phase with each other. The reason for this is that the other part of the velocity in Eq.4.4.3, namely, $U_\phi(r)$, is a complex entity as can be anticipated from the presence of i in its governing equation (Eq.4.4.4) and as we see in the next section. The product of this complex entity with $e^{i\omega t}$ in Eq.4.4.3 alters the phases of the real and imaginary parts of the velocity $u_\phi(r,t)$ so that in general they are not the same as those of the real and imaginary parts of the pressure gradient $k_\phi(t)$.

4.5 Solution of Bessel Equation

Equation 4.4.4 is a form of Bessel equation that has a known general solution [4,5], namely,

$$U_\phi(r) = \frac{ik_s a^2}{\mu\Omega^2} + AJ_0(\zeta) + BY_0(\zeta) \tag{4.5.1}$$

where A, B are arbitrary constants and J_0, Y_0 are Bessel functions of order zero and of the first and second kind, respectively (Figs.4.5.1,2), satisfying

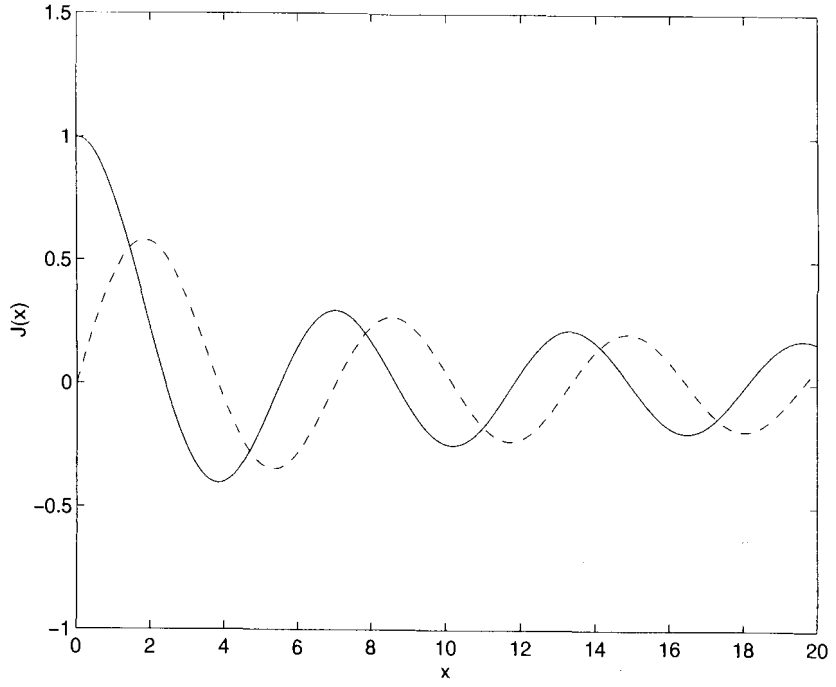

FIGURE 4.5.1. Bessel functions of the first kind, of order zero [$J_0(x)$, solid line] and order one [$J_1(x)$, dashed line], where x is real.

the standard Bessel equation

$$\frac{d^2J_0}{d\zeta^2} + \frac{1}{\zeta}\frac{dJ_0}{d\zeta} + J_0 = 0 \tag{4.5.2}$$

$$\frac{d^2Y_0}{d\zeta^2} + \frac{1}{\zeta}\frac{dY_0}{d\zeta} + Y_0 = 0 \tag{4.5.3}$$

The new variable ζ is a complex variable related to the radial coordinate r by

$$\zeta(r) = \Lambda\frac{r}{a} \tag{4.5.4}$$

where Λ is a complex frequency parameter related to the nondimensional frequency Ω by

$$\Lambda = \left(\frac{i-1}{\sqrt{2}}\right)\Omega \tag{4.5.5}$$

Because of this relation, and because Λ and Ω appear explicitly and implicitly in all elements of the solution, the numerical value of the nondimensional frequency Ω has a key effect on the detailed characteristics of the flow field.

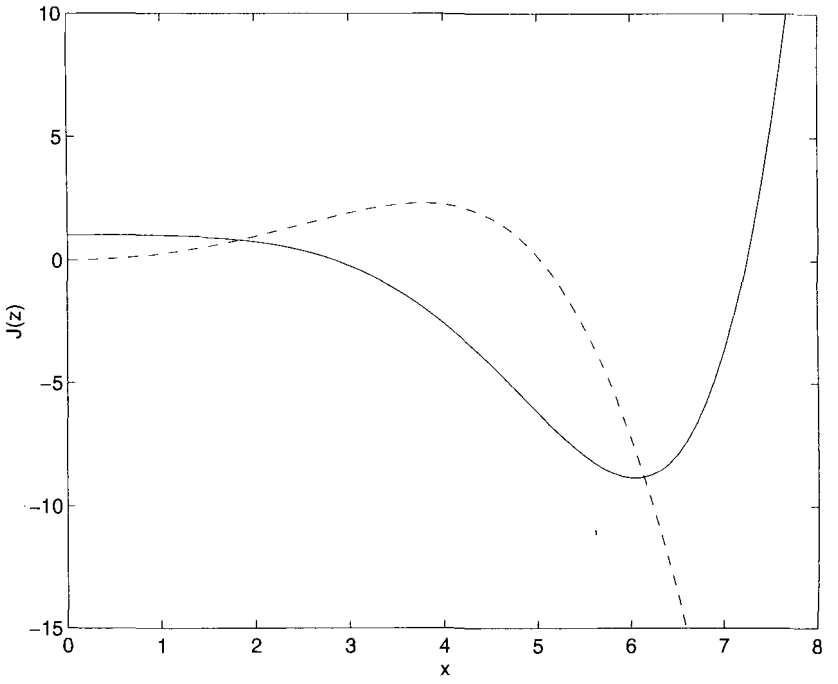

FIGURE 4.5.2. Real part (solid line) and imaginary part (dashed line) of $J_0(z)$, where $z = (i-1)x/2^{1/2}$.

Substituting the solution (Eq.4.5.1) into the governing equation (Eq.4.4.4) readily verifies that the governing equation is satisfied. In fact, it can be readily verified that the first term on the right-hand side of Eq.4.5.1 represents a particular solution of Eq.4.4.4 since it satisfies that equation and it does not contain an arbitrary constant. Then it can be verified that each of the second and third terms on the right-hand side of Eq.4.5.1 satisfies the *homogeneous* form of the governing equation, that is,

$$\frac{d^2U_\phi}{dr^2} + \frac{1}{r}\frac{dU_\phi}{dr} - \frac{i\Omega^2}{a^2}U_\phi = 0 \tag{4.5.6}$$

Substituting $U_\phi = AJ_0$ into this equation produces Eq.4.5.2, which is known to be valid by definition of J_0, and similarly for Y_0. Furthermore, it is known from the properties of J_0 and Y_0 that they are *independent* of each other, that is, one cannot be expressed in terms of the other. Therefore the three terms on the right-hand side of Eq.4.5.1 represent the required elements of the general solution of Eq.4.4.4, namely, two independent solutions of the homogeneous equation (Eq.4.5.6) and a particular solution of the full equation (Eq.4.4.4).

The boundary conditions that the solution must satisfy for flow in a tube are no-slip at the tube wall and finite velocity along the axis of the tube,

that is,

$$U_\phi(a) = 0 \tag{4.5.7}$$

$$|U_\phi(0)| < \infty \tag{4.5.8}$$

These provide the required conditions for determining the constants A, B in the solution. It is known from the properties of $Y_0(\zeta)$ that it becomes infinite as $\zeta \to 0$ [4,5], which occurs on the axis of the tube where $r = 0$, thus the boundary condition in Eq.4.5.8 leads to

$$B = 0 \tag{4.5.9}$$

and the first boundary condition then gives

$$A = \frac{-ik_s a^2}{\mu\Omega^2 J_0(\Lambda)} \tag{4.5.10}$$

noting from Eq.4.5.4 that

$$\zeta(a) = \Lambda \tag{4.5.11}$$

With these values of A, B the solution for U_ϕ is finally

$$U_\phi = \frac{ik_s a^2}{\mu\Omega^2}\left(1 - \frac{J_0(\zeta)}{J_0(\Lambda)}\right) \tag{4.5.12}$$

4.6 Oscillatory Velocity Profiles

The solution of Eq.4.4.2 for the oscillatory flow velocity $u_\phi(r,t)$ is now complete. Using Eqs.4.4.3 and 4.5.12, we have

$$u_\phi(r,t) = \frac{ik_s a^2}{\mu\Omega^2}\left(1 - \frac{J_0(\zeta)}{J_0(\Lambda)}\right) e^{i\omega t} \tag{4.6.1}$$

This is a classical solution for oscillatory flow in a rigid tube, obtained in different forms and at different times by Sexl [6], Womersley [7], Uchida [8], and discussed at some length by McDonald [9] and Milnor [10].

The first element of the solution is a constant coefficient whose value depends on the amplitude of the pressure gradient k_s, radius of the tube a, viscosity of the fluid μ, and the frequency of oscillation Ω. The second element, inside the large parentheses, is a function of r that describes the velocity profile in a cross section of the tube. The third element is a function of time, which multiplies and therefore modifies the velocity profile as time changes within the oscillatory cycle, thus producing a sequence of oscillatory velocity profiles.

To compare these oscillatory profiles with the constant parabolic profile in Poiseuille flow, we consider steady and oscillatory flows in tubes of the same radius a, and take k_s in Eq.4.6.1 to be both the constant pressure gradient in the Poiseuille flow case and the *amplitude* of the oscillatory pressure gradient in the oscillatory flow case. To further facilitate the comparison, the oscillatory flow velocity $u_\phi(r,t)$ is divided by the maximum velocity in Poiseuille flow $\hat{u}_s$, using Eqs.3.4.1 and 4.5.5, to get

$$\frac{u_\phi(r,t)}{\hat{u}_s} = \frac{-4}{\Lambda^2}\left(1 - \frac{J_0(\zeta)}{J_0(\Lambda)}\right) e^{i\omega t} \tag{4.6.2}$$

This nondimensional form of the oscillatory velocity has the convenient scale in which a value of 1.0 represents a velocity equal to the maximum velocity in the corresponding Poiseuille flow case.

Because of the complex form of the driving pressure gradient (Eq.4.4.1) for which the solution was obtained, Eq.4.6.2 above actually represents two distinct solutions: one for which the pressure gradient varies as the real part of k_ϕ, namely, $\cos\omega t$, and another for which the gradient varies as the imaginary part of k_ϕ, namely, $\sin\omega t$. It is convenient to introduce the following notation for the real and imaginary parts of the velocity and

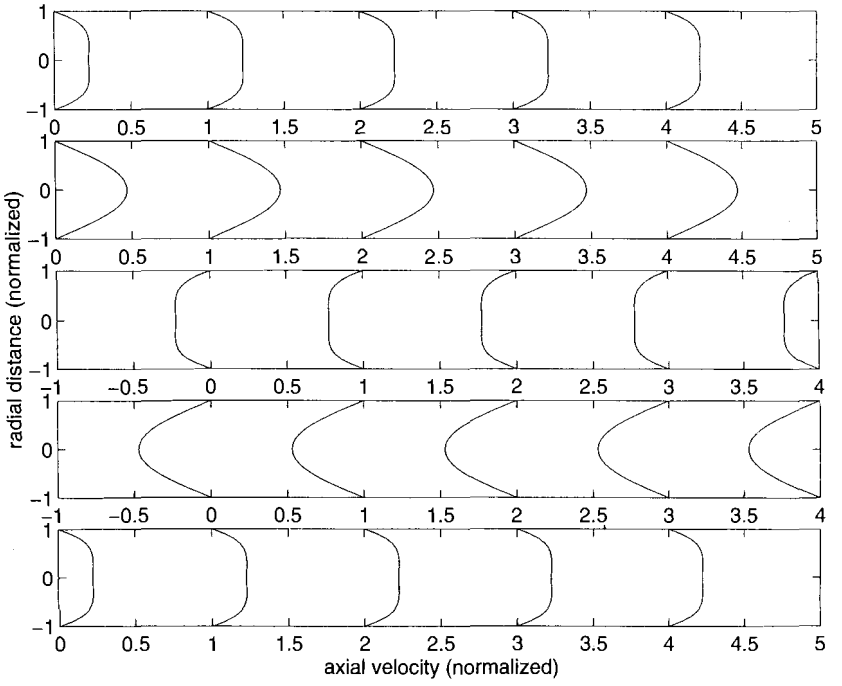

FIGURE 4.6.1. Oscillatory velocity profiles in a rigid tube with frequency parameter $\Omega = 3.0$ and corresponding to the *real* part of the pressure gradient, namely, $k_s \cos\omega t$. The panels represent the profiles at different phase angles (ωt) within the oscillatory cycle, with $\omega t = 0$ in the top panel then increasing by 90° for subsequent panels.

pressure:

$$k_\phi = k_{\phi R} + ik_{\phi I} \tag{4.6.3}$$

$$= k_s(\cos\omega t + i\sin\omega t) \tag{4.6.4}$$

thus

$$k_{\phi R} = k_s\cos\omega t, \quad k_{\phi I} = k_s\sin\omega t \tag{4.6.5}$$

The corresponding velocities are the real and imaginary parts of u_ϕ, that is,

$$u_\phi = u_{\phi R} + iu_{\phi I} = U_\phi e^{i\omega t} \tag{4.6.6}$$

$$= U_\phi(\cos\omega t + i\sin\omega t) \tag{4.6.7}$$

It is important to note that the real and imaginary parts of the velocity *do not* vary as $\cos\omega t$ and $\sin\omega t$ because in the expression for U_ϕ (Eq.4.5.12) the quantities $\Lambda, \zeta, J_0(\zeta), J_0(\Lambda)$ are all complex. Thus the real and imaginary parts of the velocity in these expressions are generally different from those of the pressure gradient, hence a phase difference exists between the oscillatory pressure gradient and the oscillatory velocity profiles that it produces.

If the real and imaginary parts of U_ϕ are denoted by $U_{\phi R}$ and $U_{\phi I}$, respectively, that is,

$$\frac{U_{\phi R}}{\hat{u}_s} = \Re\left\{\frac{-4}{\Lambda^2}\left(1 - \frac{J_0(\zeta)}{J_0(\Lambda)}\right)\right\} \tag{4.6.8}$$

$$\frac{U_{\phi I}}{\hat{u}_s} = \Im\left\{\frac{-4}{\Lambda^2}\left(1 - \frac{J_0(\zeta)}{J_0(\Lambda)}\right)\right\} \tag{4.6.9}$$

and

$$U_\phi = U_{\phi R} + iU_{\phi I} \tag{4.6.10}$$

then Eq.4.6.7 becomes

$$u_\phi = (U_{\phi R} + iU_{\phi I})(\cos\omega t + i\sin\omega t) \tag{4.6.11}$$

and the real and imaginary parts of u_ϕ are given by

$$u_{\phi R} = U_{\phi R}\cos\omega t - U_{\phi I}\sin\omega t \tag{4.6.12}$$

$$u_{\phi I} = U_{\phi I}\cos\omega t + U_{\phi R}\sin\omega t \tag{4.6.13}$$

To facilitate the computation of the real or imaginary parts of the velocity, tables of the complex values of $J_0(\zeta)$ are provided in Appendix A.

It is clear from the expressions in Eq.4.6.1 that the shape of the oscillatory velocity profiles will depend critically on the frequency of oscillation ω, since ω determines the values of the nondimensional frequency Ω, the complex frequency Λ, the complex variable ζ, and ultimately the Bessel function J_0 and oscillatory flow velocity u_ϕ. A set of oscillatory velocity profiles corresponding to $\Omega = 3$ and to the *real* part of the pressure gradient, namely, $k_s\cos\omega t$, is shown in Fig.4.6.1.

It is observed that velocity profiles oscillate between a peak profile in the forward direction and a peak profile in the backward direction, but neither the phase nor amplitude of these peak profiles correspond with the peaks of the oscillatory pressure. The first because forward and backward peaks of the pressure gradient, being $k_s\cos\omega t$, occur at $\omega t = 0°, 180°$, while the corresponding peak velocity profiles are seen to occur at approximately $\omega t = 90°, 270°$. Thus the oscillatory velocity *lags* the oscillatory pressure, clearly because of the inertia of the fluid. The second because maximum velocity in the peak velocity profile is less than 1.0, which means that it is less than the maximum velocity in the corresponding Poiseuille profile.

4.7 Oscillatory Flow Rate

Volumetric flow rate q_ϕ in oscillatory flow through a tube is obtained by integrating the oscillatory velocity profile over a cross section of the tube. Since the oscillatory velocity $u_\phi(r,t)$ is a function of r and t, the result is a function of time given by

$$q_\phi(t) = \int_0^a 2\pi r u_\phi(r,t)dr \tag{4.7.1}$$

Using the solution for $u_\phi(r,t)$ in Eq.4.6.1, this becomes

$$q_\phi(t) = \frac{2\pi i k_s a^2}{\mu\Omega^2}e^{i\omega t}\int_0^a r\left(1 - \frac{J_0(\zeta)}{J_0(\Lambda)}\right)dr \tag{4.7.2}$$

The integral on the right-hand side is evaluated as follows:

$$\int_0^a r\left(1 - \frac{J_0(\zeta)}{J_0(\Lambda)}\right)dr = \frac{a^2}{\Lambda^2 J_0(\Lambda)}\int_0^\Lambda (J_0(\Lambda) - J_0(\zeta))\zeta d\zeta$$

$$= \frac{a^2}{2}\left(1 - \frac{2J_1(\Lambda)}{\Lambda J_0(\Lambda)}\right) \tag{4.7.3}$$

where J_1 is a Bessel function of the first order and first kind, related to J_0 by

$$\int \zeta J_0(\zeta)d\zeta = \zeta J_1(\zeta) \tag{4.7.4}$$

Thus the oscillatory flow rate is finally given by

$$q_\phi(t) = \frac{i\pi k_s a^4}{\mu\Omega^2}\left(1 - \frac{2J_1(\Lambda)}{\Lambda J_0(\Lambda)}\right)e^{i\omega t} \tag{4.7.5}$$

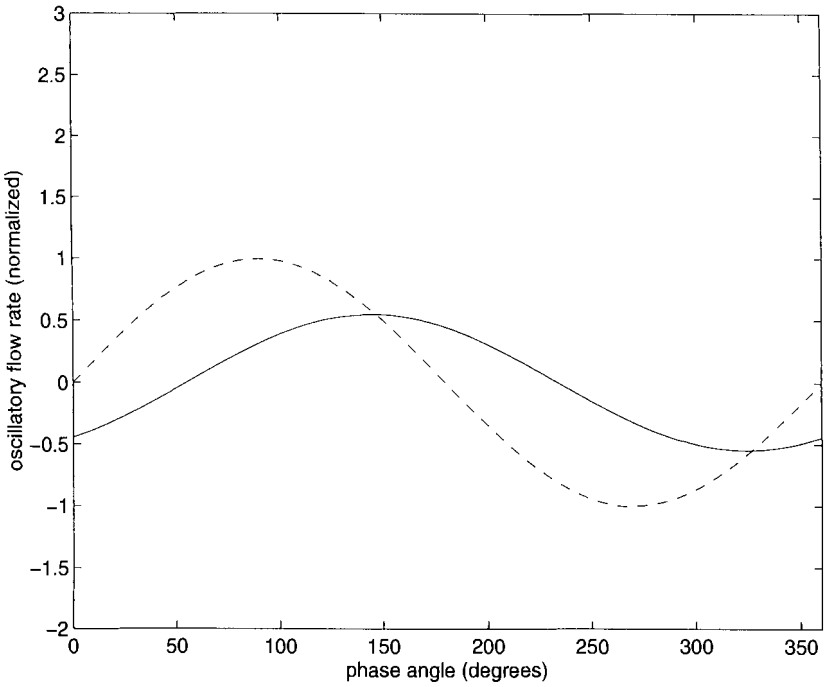

FIGURE 4.7.1. Variation of the oscillatory flow rate q_ϕ within an oscillatory cycle (solid line), compared with variation of the corresponding pressure gradient, in this case $k_{\phi I} = k_s \sin \omega t$ (dashed line). Peak flow occurs later than peak pressure, that is, the flow wave *lags* the pressure wave. Also, normalized peak flow is less than 1.0, which means that peak flow is less than the corresponding Poiseuille flow rate under the same pressure gradient.

The net flow rate Q_ϕ over one oscillatory cycle is given by

$$\begin{aligned} Q_\phi &= \int_0^T q_\phi(t)dt \\ &= \frac{i\pi k_s a^4}{\mu\Omega^2}\left(1 - \frac{2J_1(\Lambda)}{\Lambda J_0(\Lambda)}\right)\int_0^T (\cos\omega t + i\sin\omega t)dt \\ &= \frac{i\pi k_s a^4}{\mu\Omega^2}\left(1 - \frac{2J_1(\Lambda)}{\Lambda J_0(\Lambda)}\right)\int_0^{2\pi} (\cos\theta + i\sin\theta)d\theta \\ &= 0 \end{aligned} \tag{4.7.6}$$

where $T = 2\pi/\omega$ is the period of oscillation. The result confirms that in oscillatory flow the fluid moves only back and forth, with no net flow in either direction.

To examine the variation of flow rate within the oscillatory cycle, it is convenient to put Eq.4.7.5 into nondimensional form, as was done for the velocity in the previous section. Dividing Eq.4.7.5 through by the corresponding flow rate in steady Poiseuille flow, namely, q_s in Eq.3.4.3, gives

$$\frac{q_\phi(t)}{q_s} = \frac{-8}{\Lambda^2}\left(1 - \frac{2J_1(\Lambda)}{\Lambda J_0(\Lambda)}\right)e^{i\omega t} \tag{4.7.7}$$

The ratio represents the oscillatory flow rate scaled in terms of the corresponding flow rate in Poiseuille flow, thus a value of 1.0 represents a flow rate equal to that in Poiseuille flow in the same tube and under a constant pressure gradient equal to k_s. Numerical computations require values of $J_1(\Lambda)$ in addition to those of $J_0(\Lambda)$. A table of these is given in Appendix A. It is clear from the expression on the right-hand side of Eq.4.7.7 that the oscillatory flow rate depends heavily on the frequency of oscillation. It should also be noted that the expression is *complex*, its real part corresponding to the real part of the pressure gradient, and its imaginary part corresponding to the imaginary part of the pressure gradient.

Variation of $q_\phi(t)/q_s$ over one oscillatory cycle, at a moderate frequency, $\Omega = 3.0$, is shown in Fig.4.7.1. It is seen that the flow rate oscillates between a peak in the forward direction and a peak in the backward direction. At this frequency the value of the peak is decidedly less than 1.0, which means that the flow rate falls short of reaching the corresponding flow rate in Poiseuille flow under a constant pressure gradient equal to k_s, which is the peak value of the oscillatory pressure gradient. The reason for this is clearly the inertia of the fluid, which must be accelerated to peak flow in each cycle. We shall see later that this effect intensifies as the frequency of oscillation increases, the fluid having greater and greater difficulty reaching a peak flow commensurate with that in Poiseuille flow.

4.8 Oscillatory Shear Stress

In oscillatory flow, as fluid moves back and forth in response to the oscillatory pressure gradient, the shear stress exerted by the fluid on the tube wall varies accordingly as a function of time given by

$$\tau_\phi(t) = -\mu\left(\frac{\partial u_\phi(r,t)}{\partial r}\right)_{r=a} \tag{4.8.1}$$

It is important to note that, since this shear is produced by only the oscillatory velocity u_ϕ, it is *in addition* to that produced by the steady velocity u_s when present.

Using the solution for $u_\phi(r,t)$ in Eq.4.6.1, this becomes

$$\tau_\phi(t) = -\frac{ik_s a^2}{\Omega^2}\left\{\frac{d}{dr}\left(1 - \frac{J_0(\zeta)}{J_0(\Lambda)}\right)\right\}_{r=a} e^{i\omega t}$$

$$= -\frac{ik_s a^2}{\Omega^2}\left\{\frac{d}{d\zeta}\left(1-\frac{J_0(\zeta)}{J_0(\Lambda)}\right)\right\}_{\zeta=\Lambda}\frac{\Lambda}{a}e^{i\omega t}$$

$$= -\frac{k_s a}{\Lambda}\left(\frac{J_1(\Lambda)}{J_0(\Lambda)}\right)e^{i\omega t} \qquad (4.8.2)$$

where the relations between ζ,Λ and Ω in Eqs.4.5.4,5 have been used, as well as the following relation between Bessel functions of the first and zeroth order [4,5]:

$$\frac{dJ_0(\zeta)}{d\zeta} = -J_1(\zeta) \qquad (4.8.3)$$

As before, it is convenient to put Eq.4.8.2 into nondimensional form by scaling the oscillatory shear stress by the corresponding shear stress in Poiseuille flow, that is, by dividing through by τ_s as given in Eq.3.4.6, to get

$$\frac{\tau_\phi(t)}{\tau_s} = \frac{2}{\Lambda}\left(\frac{J_1(\Lambda)}{J_0(\Lambda)}\right)e^{i\omega t} \qquad (4.8.4)$$

The expression on the right-hand side is complex, its real part representing the shear stress at the tube wall when the driving pressure gradient varies as $\cos\omega t$ and its imaginary part representing that shear when the gradient varies as $\sin\omega t$. In both cases the result is numerically scaled by the corresponding shear stress in Poiseuille flow.

Variation of the imaginary part of $\tau_\phi(t)$ within the oscillatory cycle is shown in Fig.4.8.1. It is seen that it has a sinusoidal form like that of the imaginary part of the pressure gradient driving the flow, but with a phase difference between the two. The oscillatory shear stress lags the pressure, somewhat like the oscillatory flow rate. The amplitude of the oscillatory shear indicates the highest shear stress reached at the peak of each cycle as the fluid moves back and forth in each direction. This maximum clearly depends heavily on the frequency of oscillation as evident from Eq.4.8.4. The results shown in Fig.4.8.1 are for $\Omega = 3.0$, where it is seen that the oscillatory shear reaches a maximum value at the peak of each cycle of approximately one half the steady Poiseuille flow value.

In pulsatile flow consisting of steady- and oscillatory-flow components, the oscillatory shear stress adds to and subtracts from the steady shear stress. The results in Fig.4.8.1 show that in pulsatile flow at this particular frequency the shear stress would oscillate between a high of approximately 1.5 to a low of approximately 0.5 times its constant value in steady Poiseuille flow.

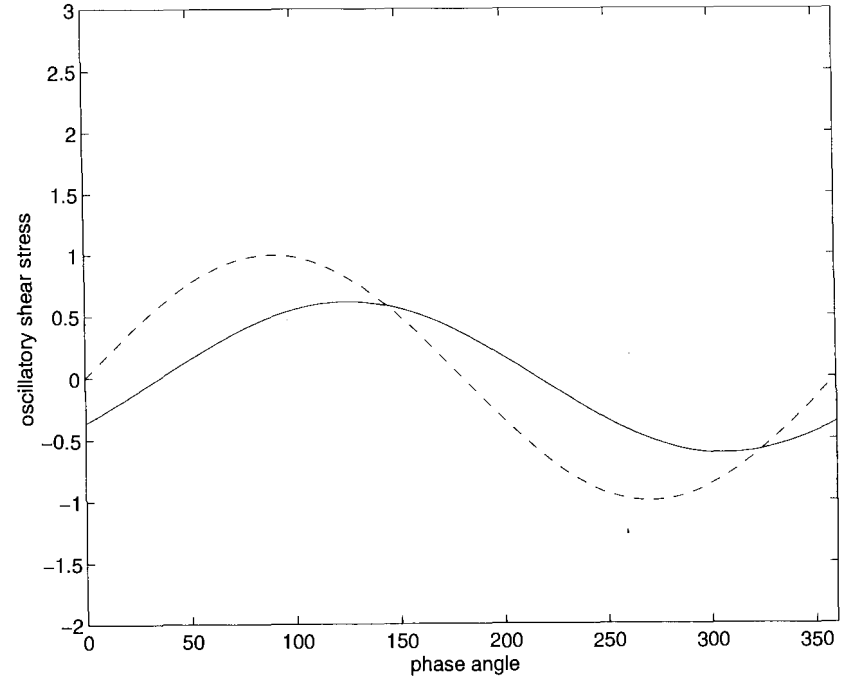

FIGURE 4.8.1. Variation of the imaginary part of oscillatory shear stress $\tau_{\phi I}$ (solid line) compared with the corresponding part of the pressure gradient $k_{\phi I}$ (dashed line). Shear stress *lags* the pressure, and its normalized value at its peak is less than 1.0, hence less than the corresponding shear stress in Poiseuille flow. Because the shear stress shown here is produced entirely by the oscillatory flow, it is *in addition* to the constant shear stress produced by the steady component of pulsatile flow.

4.9 Pumping Power

As in the case of steady Poiseuille flow, in pulsatile flow the equation governing the flow can be used to examine the balance of energy expenditure and in particular, in this case, to determine the pumping power required to drive the flow. Since the oscillatory part of pulsatile flow does not produce any net flow forward, and since the pumping power required to drive the steady part of pulsatile flow is the same as that in steady flow, any power expenditure on the oscillatory part of the flow is an "added expense" that reduces the efficiency of the flow. In this section we examine this added expense by considering the balance of energy expenditures in oscillatory flow, much along the same lines as was done for steady flow in Section 3.5.

We begin with the governing equation for oscillatory flow, namely, Eq.4.2.7

$$\mu\left(\frac{\partial^2 u_\phi}{\partial r^2}+\frac{1}{r}\frac{\partial u_\phi}{\partial r}\right)-\rho\frac{\partial u_\phi}{\partial t}=k_\phi(t)$$

For the purpose of present discussion we recall that in this equation both the velocity and pressure are complex quantities and that, therefore, the equation actually governs two separate problems, one for the real parts and one for the imaginary parts of the velocity and pressure. Using the notation of Section 4.6, the two governing equations are

$$\mu\left(\frac{\partial^2 u_{\phi R}}{\partial r^2}+\frac{1}{r}\frac{\partial u_{\phi R}}{\partial r}\right)-\rho\frac{\partial u_{\phi R}}{\partial t}=k_{\phi R} \tag{4.9.1}$$

$$\mu\left(\frac{\partial^2 u_{\phi I}}{\partial r^2}+\frac{1}{r}\frac{\partial u_{\phi I}}{\partial r}\right)-\rho\frac{\partial u_{\phi I}}{\partial t}=k_{\phi I} \tag{4.9.2}$$

Discussion of energy expenditure is more meaningful in terms of one or the other of these two equations, rather than in terms of the equation in complex form (Eq.4.2.7). Accordingly, the present discussion shall be based on Eq.4.9.2 that corresponds to an oscillatory pressure gradient varying as $\sin\omega t$, which was used in other sections in the present chapter. Similar discussion with obvious modifications can be based on Eq.4.9.1.

As in the case of steady Poiseuille flow, Eq.4.9.2 as it stands represents a balance of *forces per unit volume*. In the steady case this balance is between only the driving pressure term on the right-hand side and the viscous resistance term on the left-hand side. In the present case, however, there is an added acceleration term on the left-hand side. At any point in time, in oscillatory flow, the driving pressure force must equal the *net* sum of viscous and acceleration forces that may add to or subtract from each other at different times within the oscillatory cycle.

As in Section 3.5, we consider a specific volume of fluid consisting of a cylindrical shell of radius r, length l, and thickness dr, moving with velocity $u_{\phi I}(r,t)$. It is important to recall that axial location x along the tube is not a factor in pulsatile flow through a rigid tube because fluid at all cross sections of the tube is moving with the same velocity profile, hence x does not appear as a variable in the velocity or in the governing equation.

If each of the three terms in Eq.4.9.2 is multiplied by the volume of this cylindrical shell of fluid, namely, $2\pi rldr$, and by the velocity $u_{\phi I}$, the result is an equation governing the balance of energy expenditures associated with this volume of fluid. Writing

$$dH_{vI} = \mu\left(\frac{\partial^2 u_{\phi I}}{\partial r^2}+\frac{1}{r}\frac{\partial u_{\phi I}}{\partial r}\right)\times 2\pi rlu_{\phi I}dr \tag{4.9.3}$$

$$dH_{aI} = \rho\frac{\partial u_{\phi I}}{\partial t}\times 2\pi rlu_{\phi I}dr \tag{4.9.4}$$

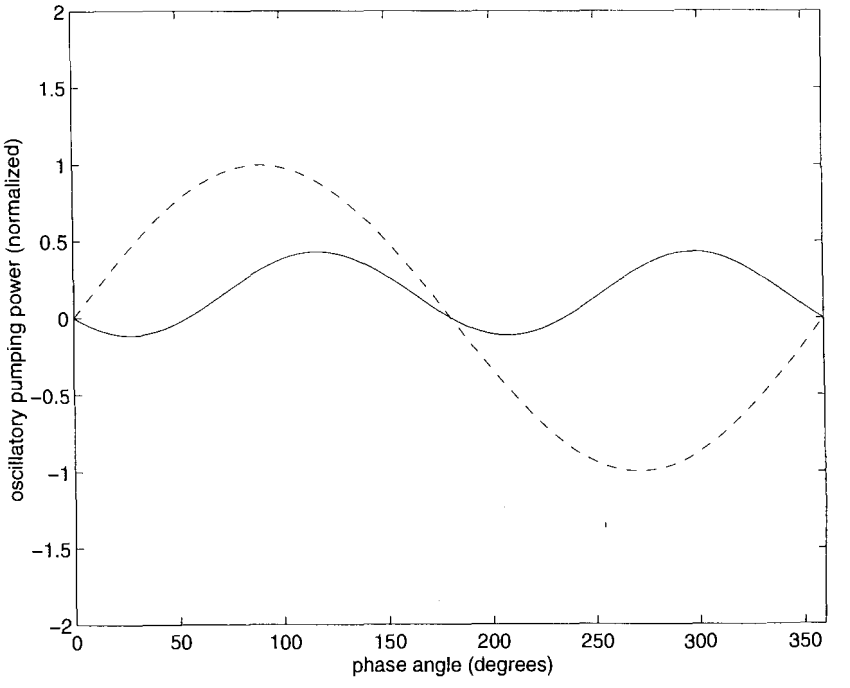

FIGURE 4.9.1. Variation of oscillatory pumping power $H_{\phi I}$ during one cycle (solid line) compared with the corresponding pressure gradient $k_{\phi I}$ (dashed line). The power has two peaks within each oscillatory cycle because it consists of the product of oscillatory pressure and oscillatory flow. The integral of the power over one cycle is not zero, hence oscillatory flow requires energy to maintain even though the net flow is zero. This energy expenditure is required to maintain the energy dissipation at the tube wall. The net energy expenditure for accelerating and decelerating the flow is zero (see text).

$$dH_{pI} = k_{\phi I}\times 2\pi rlu_{\phi I}dr \tag{4.9.5}$$

Eq.4.9.2 becomes

$$dH_{vI}(r,t)-dH_{aI}(r,t)=dH_{pI}(r,t) \tag{4.9.6}$$

The notation emphasizes the fact that each term is a function of r and t, and that the imaginary parts of the velocity and pressure are being used for illustration. Subscripts v,a,p are used to associate energy expenditure with viscous dissipation, acceleration, and pressure, respectively. If now each term is integrated over a cross section of the tube as was done in the steady flow case, the r dependence is removed and the equation then becomes a balance of energy expenditure for a cylindrical volume of fluid of radius a and length l filling the entire cross section of the tube. If the results of integration are denoted by H_v, H_a, H_p, respectively, the equation

becomes

$$H_{vI}(t) - H_{aI}(t) = H_{pI}(t) \tag{4.9.7}$$

where, for each term,

$$H(t) = \int_{r=0}^{r=a} dH(r,t) \tag{4.9.8}$$

Eq.4.9.7 expresses the balance of energy expenditures *at each point in time* within the oscillatory cycle.

If each term in Eq.4.9.7 is now integrated in time over one cycle of period $T = 2\pi/\omega$, and if we denote the results by E_v, E_a, E_p, respectively, then the equation becomes

$$E_v - E_a = E_p \tag{4.9.9}$$

where, for each term,

$$E = \int_0^T H(t)dt \tag{4.9.10}$$

Eq.4.9.9 expresses the balance of energy expenditures *over one complete oscillatory cycle*, a real/imaginary subscript is not required since the equation holds in both cases.

At a particular point in time within the oscillatory cycle, the viscous component of the energy expenditure, using Eq.4.9.3, is given by

$$\begin{aligned} H_{vI}(t) &= \int_{r=0}^{r=a} dH_{vI}(r,t) \\ &= 2\pi\mu l \int_0^a u_{\phi I}\left(\frac{\partial^2 u_{\phi I}}{\partial r^2} + \frac{1}{r}\frac{\partial u_{\phi I}}{\partial r}\right) r dr \\ &= 2\pi\mu l \int_{r=0}^{r=a} u_{\phi I}\frac{\partial}{\partial r}\left(r\frac{\partial u_{\phi I}}{\partial r}\right) dr \\ &= 2\pi\mu l \left| u_{\phi I}\frac{\partial u_{\phi I}}{\partial r} r \right|_{r=0}^{r=a} - \int_{r=0}^{r=a} \frac{\partial u_{\phi I}}{\partial r} r du_{\phi I} \\ &= -2\pi\mu l \int_0^a \left(\frac{\partial u_{\phi I}}{\partial r}\right)^2 r dr \end{aligned} \tag{4.9.11}$$

which, as in the case of steady flow, represents the rate of energy expenditure due to viscous dissipation. And because this dissipation is due to the oscillatory velocity component $u_{\phi I}$, this energy expenditure is due entirely to the oscillatory component of the flow.

The accelerating component of energy expenditure, using Eq.4.9.4, is given by

$$\begin{aligned} H_{aI}(t) &= \int_{r=0}^{r=a} dH_{aI}(r,t) \\ &= 2\pi\rho l \int_0^a u_{\phi I}\left(\frac{\partial u_{\phi I}}{\partial t}\right) r dr \\ &= 2\pi\rho l \int_0^a \frac{\partial}{\partial t}\left(\frac{u_{\phi I}^2}{2}\right) r dr \\ &= 2\pi l \frac{d}{dt}\int_0^a \left(\frac{1}{2}\rho u_{\phi I}^2\right) r dr \end{aligned} \tag{4.9.12}$$

which represents the rate of energy expenditure required for accelerating the flow, increasing its kinetic energy as indicated under the integral sign.

The driving (pressure) component of energy expenditure, using Eq.4.9.5, is given by

$$\begin{aligned} H_{pI}(t) &= \int_{r=0}^{r=a} dH_{pI}(t) \\ &= lk_{\phi I}\int_0^a 2\pi r u_{\phi I} dr \\ &= lk_{\phi I} q_{\phi I} \end{aligned} \tag{4.9.13}$$

which represents the pumping power required to drive the flow and where $q_{\phi I}$ is the imaginary part of the flow rate, from Eq.4.7.5

$$q_{\phi I} = \Im\left\{\frac{i\pi k_s a^4}{\mu\Omega^2}\left(1 - \frac{2J_1(\Lambda)}{\Lambda J_0(\Lambda)}\right) e^{i\omega t}\right\} \tag{4.9.14}$$

Thus the *instantaneous* balance of energy expenditure, by substituting into Eq.4.9.7 from Eqs.4.9.11–13, can be written as

$$\begin{aligned} -2\pi\mu l \int_0^a r\left(\frac{\partial u_{\phi I}}{\partial r}\right)^2 dr + 2\pi l \frac{d}{dt}\int_0^a \left(\frac{1}{2}\rho u_{\phi I}^2\right) r dr \\ = lk_{\phi I} q_{\phi I} \end{aligned} \tag{4.9.15}$$

from which it is seen that, at any point in time, the pumping power on the right-hand side is being expended on the net sum of energy required to accelerate the flow and that required to overcome the viscous resistance. Since as the oscillatory cycle progresses the acceleration term changes sign while the viscous term does not, the net result at any instant may represent the sum or difference of the two terms. Physically, this means that during the acceleration phase of the oscillatory cycle the pumping power pays for both acceleration and viscous dissipation, while during the deceleration phase the flow actually returns some of its kinetic energy.

It should be noted that if the pumping power is to be defined as a *positive* quantity as was done for steady flow (Eq.3.4.14), then we introduce

$$H_{\phi I}(t) = -lk_{\phi I} q_{\phi I} = -H_{pI} \tag{4.9.16}$$

$$H_{\phi R}(t) = -lk_{\phi R}q_{\phi R} = -H_{pR} \tag{4.9.17}$$

Variation of oscillatory pumping power is shown in Fig.4.9.1, where it is seen that the power has two peaks within one oscillatory cycle because it consists of the product of k_ϕ and q_ϕ. The figure also shows clearly that the integral of the power over one cycle is not zero.

By contrast, the energy expenditure for accelerating and decelerating the flow over one cycle, if $T = 2\pi/\omega$ is the period of oscillation, is given by

$$\begin{aligned}
E_a &= \int_0^T e_a(t)dt \\
&= 2\pi\rho l \int_0^{2\pi/\omega}\int_0^a u_{\phi I}\frac{\partial u_{\phi I}}{\partial t} r dr dt \\
&= 2\pi\rho l \int_0^a \int_0^{2\pi/\omega} u_{\phi I}\frac{\partial u_{\phi I}}{\partial t} dt r dr \\
&= 2\pi\rho l \int_0^a \left\{\int_{t=0}^{t=2\pi/\omega} d\left(\frac{u_{\phi I}^2}{2}\right)\right\} r dr \\
&= 2\pi\rho l \int_0^a \left|\frac{u_{\phi I}^2}{2}\right|_{t=0}^{t=2\pi/\omega} r dr \\
&= 2\pi\rho l \int_0^a \left|\frac{(U_{\phi I}\cos\omega t + U_{\phi R}\sin\omega t)^2}{2}\right|_{t=0}^{t=2\pi/\omega} r dr \\
&= 0
\end{aligned} \tag{4.9.18}$$

Thus while the instantaneous energy expenditure $H_a(t)$ required to accelerate the flow is generally nonzero, the net expenditure over one cycle is zero. The energy spent during one half of the cycle is recovered during the other half.

It follows, therefore, that *over one cycle* the average power expenditure required to drive the oscillatory part of the flow is equal to that being dissipated by viscosity, that is,

$$E_p = E_v \tag{4.9.19}$$

The *positive* average rate of energy expenditure over one cycle is thus given by

$$\frac{E_\phi}{2\pi/\omega} = \frac{1}{2\pi/\omega}\int_0^{2\pi/\omega} H_{\phi I}(t)dt = \frac{1}{2\pi/\omega}\int_0^{2\pi/\omega} H_{\phi R}(t)dt \tag{4.9.20}$$

$$= -\frac{l}{2\pi/\omega}\int_0^{2\pi/\omega} k_{\phi I}q_{\phi I}(t)dt \tag{4.9.21}$$

$$= -\frac{l}{2\pi/\omega}\int_0^{2\pi/\omega} k_{\phi R}q_{\phi R}(t)dt \tag{4.9.22}$$

and expressing this as a fraction of the corresponding pumping power in steady flow (Eq.3.4.14), we get

$$\frac{E_\phi}{H_s \times 2\pi/\omega} = \frac{1}{2\pi/\omega}\int_0^{2\pi/\omega}\left(\frac{k_{\phi I}}{k_s}\right)\left(\frac{q_{\phi I}}{q_s}\right)dt \tag{4.9.23}$$

$$= \frac{1}{2\pi/\omega}\int_0^{2\pi/\omega}\left(\frac{k_{\phi R}}{k_s}\right)\left(\frac{q_{\phi R}}{q_s}\right)dt \tag{4.9.24}$$

These results are used in the next section to assess the magnitude of this energy expenditure at high and at low frequency.

4.10 Oscillatory Flow at Low Frequency

At low frequency oscillatory flow in a tube is better able to keep pace with the changing pressure. In fact at very low frequency, or in the limit of "zero frequency," the relation between flow and pressure becomes *instantaneously* the same as in steady Poiseuille flow. That is, at each point in time within the oscillatory cycle the velocity profile is what it would be in steady Poiseuille flow under a pressure gradient equal to the value of the oscillatory pressure gradient at that instant. The situation suggests the term "oscillatory Poiseuille flow." In this section we demonstrate these features of the flow analytically and derive approximate expressions which are valid at low frequency and which are easier to use than the more general expressions involving Bessel functions.

At a frequency of 1 *cycle per second*, which is equivalent to an angular frequency of 2π *radians per second*, density of 1 gm/cm^3, and viscosity of 0.04 *Poise* (*Poise* = *dyne second*/cm^2), the value of the nondimensional frequency parameter Ω, using Eq.4.4.5, is given by

$$\Omega = \sqrt{\frac{2\pi}{0.04}}\, a \tag{4.10.1}$$

where a is the radius of the tube in cm. Thus for a tube of 1 cm radius, the value of Ω is approximately 12.5. In the human system, therefore, $\Omega = 1$ may be taken as a representative low value of the frequency parameter and $\Omega = 10$ as a moderately high value.

A series expansion of the Bessel function $J_0(z)$ for small z is given by [4,5]

$$J_0(z) = 1 - \frac{z^2}{2^2} + \frac{z^4}{2^2 \times 4^2} - \frac{z^6}{2^2 \times 4^2 \times 6^2} + \ldots \tag{4.10.2}$$

The expansion is valid for *complex* values of the independent variable z as required for application to the complex solution of the pulsatile flow equation. Thus an approximation of the quotient term in Eq.4.6.2 for the velocity profile, using only the first three terms of the series, and recalling from Eq.4.5.4 that $\zeta = \Lambda r/a$, is given by

$$\begin{aligned}
\frac{J_0(\zeta)}{J_0(\Lambda)} &= \frac{J_0(\Lambda r/a)}{J_0(\Lambda)} \\
&\approx \left(1 - \frac{\Lambda^2 r^2}{4a^2} + \frac{\Lambda^4 r^4}{64a^4}\right) \times \left(1 - \frac{\Lambda^2}{4} + \frac{\Lambda^4}{64}\right)^{-1} \\
&\approx \left(1 - \frac{\Lambda^2 r^2}{4a^2} + \frac{\Lambda^4 r^4}{64a^4}\right) \times \left(1 + \frac{\Lambda^2}{4} + \frac{3\Lambda^4}{64}\right) \\
&\approx 1 + \frac{\Lambda^2}{4}\left\{\left(1 - \frac{r^2}{a^2}\right) + \frac{\Lambda^2}{16}\left(3 - \frac{4r^2}{a^2} + \frac{r^4}{a^4}\right)\right\}
\end{aligned} \tag{4.10.3}$$

only terms of order ζ^4 being retained at each step. By substituting this result into Eq.4.6.2 for the velocity profile, we obtain the following approximate expression:

$$\frac{u_\phi(r,t)}{\hat{u}_s} \approx \left\{\left(1 - \frac{r^2}{a^2}\right) - \frac{i\Omega^2}{16}\left(3 - \frac{4r^2}{a^2} + \frac{r^4}{a^4}\right)\right\} e^{i\omega t} \tag{4.10.4}$$

The real and imaginary parts of the velocity are then given by

$$\frac{u_{\phi R}(r,t)}{\hat{u}_s} \approx \left(1 - \frac{r^2}{a^2}\right)\cos\omega t + \frac{\Omega^2}{16}\left(3 - \frac{4r^2}{a^2} + \frac{r^4}{a^4}\right)\sin\omega t \tag{4.10.5}$$

$$\frac{u_{\phi I}(r,t)}{\hat{u}_s} \approx \left(1 - \frac{r^2}{a^2}\right)\sin\omega t - \frac{\Omega^2}{16}\left(3 - \frac{4r^2}{a^2} + \frac{r^4}{a^4}\right)\cos\omega t \tag{4.10.6}$$

These expressions are easier to use than Eq.4.6.2 because they do not involve Bessel functions and can be used in place of that equation when the frequency is small. Furthermore, substituting for $\hat{u}_s$ from Eq.3.4.1, and using Eq.4.6.5 for the real and imaginary parts of the pressure gradient, we obtain

$$u_{\phi R}(r,t) \approx -\frac{k_{\phi R} a^2}{4\mu}\left\{\left(1 - \frac{r^2}{a^2}\right) + \frac{\Omega^2}{16}\left(3 - \frac{4r^2}{a^2} + \frac{r^4}{a^4}\right)\tan\omega t\right\} \tag{4.10.7}$$

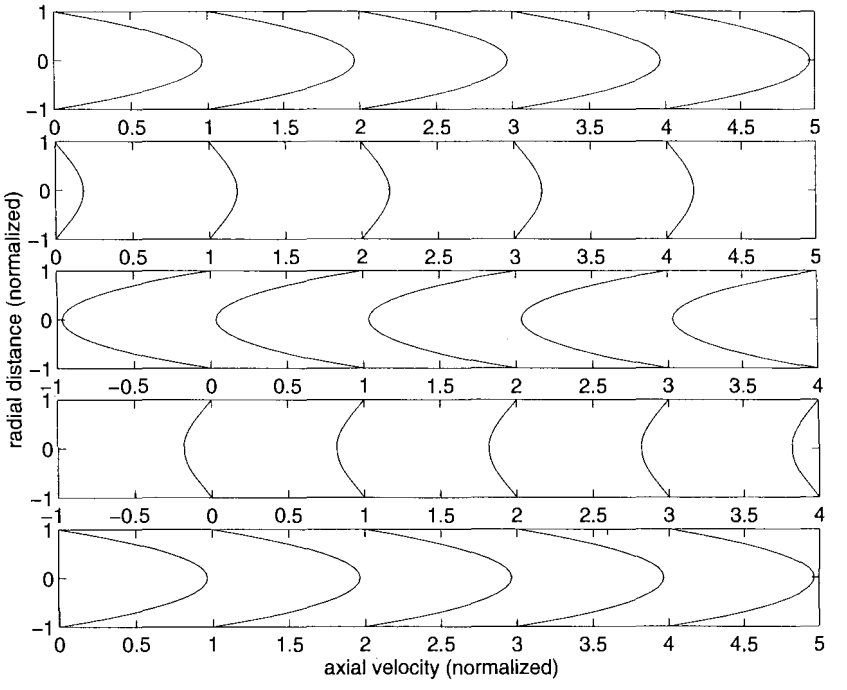

FIGURE 4.10.1. Oscillatory velocity profiles in a rigid tube at low frequency ($\Omega = 1.0$) and corresponding to the *real* part of the pressure gradient, namely, $k_s \cos\omega t$. The panels represent the profiles at different phase angles (ωt) within the oscillatory cycle, with $\omega t = 0$ in the top panel then increasing by 90° for subsequent panels. The profiles reach their peak form at the peak of pressure gradient ($\omega t = 0°, 180°$), and the maximum velocity at peak has a normalized value near 1.0. Thus flow is almost in phase with pressure gradient, and the relation between the two is as if the flow were Poiseuille flow *at each instant* (see text).

$$u_{\phi I}(r,t) \approx -\frac{k_{\phi I} a^2}{4\mu}\left\{\left(1 - \frac{r^2}{a^2}\right) - \frac{\Omega^2}{16}\left(3 - \frac{4r^2}{a^2} + \frac{r^4}{a^4}\right)\cot\omega t\right\} \tag{4.10.8}$$

We see that for small Ω where the second term in each of the two expressions can be neglected, the relation between velocity and pressure becomes

$$u_{\phi R}(r,t) \approx \frac{k_{\phi R}}{4\mu}(r^2 - a^2) \tag{4.10.9}$$

$$u_{\phi I}(r,t) \approx \frac{k_{\phi I}}{4\mu}(r^2 - a^2) \tag{4.10.10}$$

which is the same as that in Eq.3.3.10 for steady Poiseuille flow, but with instantaneous values of velocity and pressure, hence justifying the term

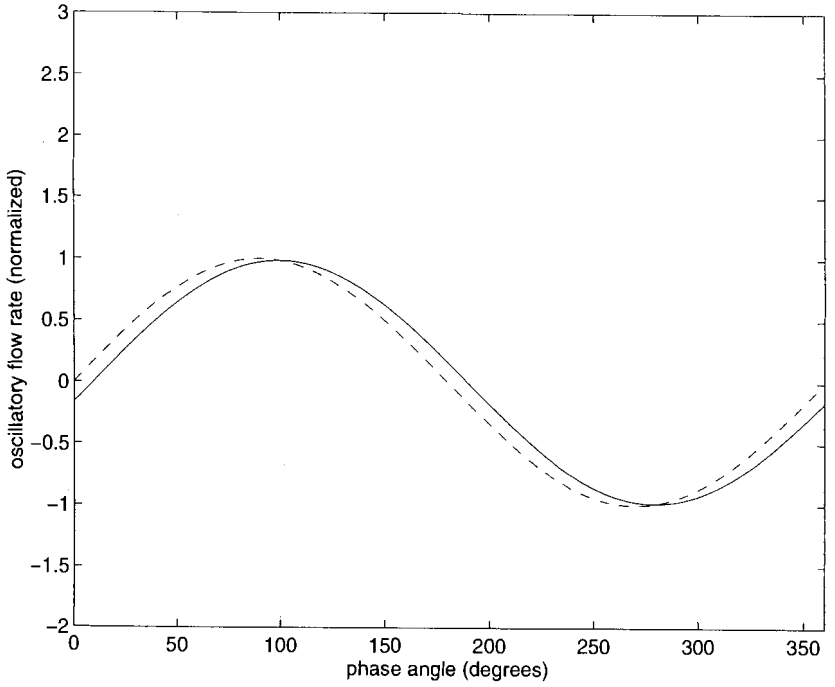

FIGURE 4.10.2. Variation of the oscillatory flow rate q_ϕ within an oscillatory cycle (solid line), compared with variation of the corresponding pressure gradient, in this case $k_{\phi I} = k_s \sin\omega t$ (dashed line), at low frequency ($\Omega = 1.0$). Flow is almost in phase with pressure gradient, and normalized peak flow is close to 1.0. Flow at each point in time is close to what it would be in steady Poiseuille flow under the instantaneous value of the pressure gradient.

"oscillatory Poiseuille flow." Velocity profiles with $\Omega = 1.0$ are shown in Fig.4.10.1.

For the flow rate we use the series expansion of $J_1(\zeta)$ for small values of ζ [4,5]:

$$J_1(\zeta) = \frac{\zeta}{2} - \frac{\zeta^3}{2^2 \times 4} + \frac{\zeta^5}{2^2 \times 4^2 \times 6} + \frac{\zeta^7}{2^2 \times 4^2 \times 6^2 \times 8} + \ldots \tag{4.10.11}$$

Using only the first three terms of the series for the quotient term in Eq.4.7.7, we find

$$\begin{aligned} \frac{J_1(\Lambda)}{J_0(\Lambda)} &\approx \frac{\Lambda}{2}\left(1 - \frac{\Lambda^2}{8} + \frac{\Lambda^4}{192}\right) \times \left(1 - \frac{\Lambda^2}{4} + \frac{\Lambda^4}{64}\right)^{-1} \\ &\approx \frac{\Lambda}{2}\left(1 - \frac{\Lambda^2}{8} + \frac{\Lambda^4}{192}\right) \times \left(1 + \frac{\Lambda^2}{4} + \frac{3\Lambda^4}{64}\right) \end{aligned}$$

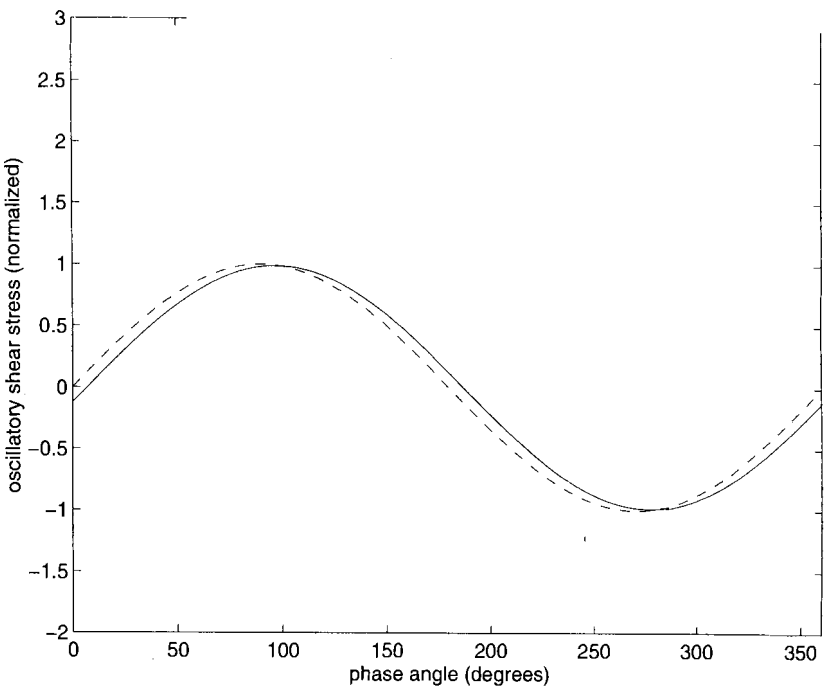

FIGURE 4.10.3. Variation of the imaginary part of oscillatory shear stress $\tau_{\phi I}$ (solid line) compared with the corresponding part of the pressure gradient $k_{\phi I}$ (dashed line), at low frequency ($\Omega = 1.0$). Shear stress is almost in phase with pressure gradient, and normalized peak shear stress is close to 1.0. Shear stress at each point in time is close to what it would be in steady Poiseuille flow under the instantaneous value of the pressure gradient.

$$\approx \frac{\Lambda}{2}\left(1 + \frac{\Lambda^2}{8} + \frac{\Lambda^4}{48}\right) \tag{4.10.12}$$

where again, only terms of order Λ^4 or lower were retained at each step. Substituting this result into Eq.4.7.7, we get

$$\frac{q_\phi(t)}{q_s} \approx \frac{8i}{\Omega^2}\left(\frac{\Lambda^2}{8} + \frac{\Lambda^4}{48}\right) e^{i\omega t} \tag{4.10.13}$$

Noting that $\Lambda^2 = -i\Omega^2$ and $\Lambda^4 = -\Omega^4$, the real and imaginary parts of the flow rate are given by

$$\frac{q_{\phi R}(t)}{q_s} \approx \cos\omega t + \frac{\Omega^2}{6}\sin\omega t \tag{4.10.14}$$

$$\frac{q_{\phi I}(t)}{q_s} \approx \sin\omega t - \frac{\Omega^2}{6}\cos\omega t \tag{4.10.15}$$

Substituting for the steady-flow rate from Eq.3.4.3, and for the real and imaginary parts of the pressure gradient from Eq.4.6.5, we get

$$q_{\phi R} \approx \frac{-k_{\phi R}\pi a^4}{8\mu}\left(1+\frac{\Omega^2}{6}\tan\omega t\right) \tag{4.10.16}$$

$$q_{\phi I} \approx \frac{-k_{\phi I}\pi a^4}{8\mu}\left(1-\frac{\Omega^2}{6}\cot\omega t\right) \tag{4.10.17}$$

At low frequency where the second term in each expression can be neglected, the relation between flow rate and pressure gradient becomes the same as that in steady flow *at each instant*, that is,

$$q_{\phi R} \approx \frac{-k_{\phi R}\pi a^4}{8\mu} \tag{4.10.18}$$

$$q_{\phi I} \approx \frac{-k_{\phi I}\pi a^4}{8\mu} \tag{4.10.19}$$

as in Eq.3.4.3 for steady flow. Flow rate with $\Omega = 1.0$ is shown in Fig.4.10.2.

In the same way, and omitting the details, we obtain the following expressions for the shear stress and maximum velocity:

$$\tau_{\phi R} \approx -\frac{k_{\phi R}a}{2}\left(1+\frac{\Omega^2}{8}\tan\omega t\right) \tag{4.10.20}$$

$$\tau_{\phi I} \approx -\frac{k_{\phi I}a}{2}\left(1-\frac{\Omega^2}{8}\cot\omega t\right) \tag{4.10.21}$$

$$\hat{u}_{\phi R} \approx \frac{-k_{\phi R}a^2}{4\mu}\left(1+\frac{3\Omega^2}{16}\tan\omega t\right) \tag{4.10.22}$$

$$\hat{u}_{\phi I} \approx \frac{-k_{\phi I}a^2}{4\mu}\left(1-\frac{3\Omega^2}{16}\cot\omega t\right) \tag{4.10.23}$$

In each case, if the frequency is low enough for the second term to be neglected, the relation becomes *instantaneously* the same as in steady flow (Eqs.3.4.1,6). If the frequency is small but not negligible, the second term can be used for approximate calculations. Oscillatory shear stress with $\Omega = 1.0$ is shown in Fig.4.10.3.

For the pumping power we have from Eqs.4.9.16,17 and the approximate results for the flow rate in Eqs.4.10.16,17

$$\begin{aligned} H_{\phi R}(t) &= -lk_{\phi R}q_{\phi R} \\ &\approx \frac{\pi a^4 l}{8\mu}k_s^2\left(\cos^2\omega t+\frac{\Omega^2}{6}\cos\omega t\sin\omega t\right) \end{aligned} \tag{4.10.24}$$

$$\begin{aligned} H_{\phi I}(t) &= -lk_{\phi I}q_{\phi I} \\ &\approx \frac{\pi a^4 l}{8\mu}k_s^2\left(\sin^2\omega t-\frac{\Omega^2}{6}\cos\omega t\sin\omega t\right) \end{aligned} \tag{4.10.25}$$

depending on whether the driving pressure gradient is the real or imaginary part of k_ϕ, respectively.

It is interesting to note that the sum of the two results is a constant independent of time and equal to the pumping power required in steady Poiseuille flow. Because the energy expenditure over one cycle is the same whether the driving pressure gradient is $k_{\phi R}$ or $k_{\phi I}$, this implies that the *average pumping power* in oscillatory flow at low frequency is one half the corresponding power in steady flow. This can be easily verified by noting that

$$\int_0^{2\pi}\cos^2\omega t d(\omega t) = \int_0^{2\pi}\sin^2\omega t d(\omega t) = \pi \tag{4.10.26}$$

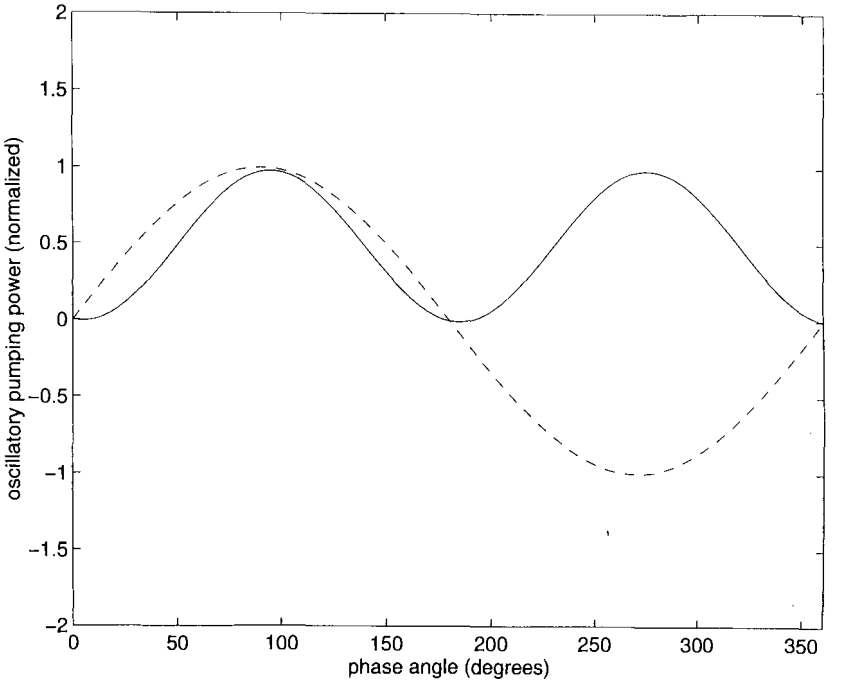

FIGURE 4.10.4. Variation of oscillatory pumping power $H_{\phi I}$ during one cycle (solid line) compared with the corresponding pressure gradient $k_{\phi I}$ (dashed line), at low frequency ($\Omega = 1.0$). The two peaks of the power coincide very closely with the peaks of pressure gradient, which at low frequency coincide with the peaks of flow rate (Fig.4.10.2). The area under the power curve, which represents the net energy expenditure over one cycle, is not zero. In fact, the area equals one half the corresponding energy expenditure in steady Poiseuille flow (see text).

while

$$\int_0^{2\pi} \cos\omega t \sin\omega t d(\omega t) = 0 \tag{4.10.27}$$

Thus whether the flow is being driven by the real or imaginary part of the pressure gradient, using Eqs.4.9.20,23,24, the average pumping power required for the oscillatory part of the flow, as a fraction of the corresponding power in steady flow, is given by

$$\frac{E_\phi}{H_s \times 2\pi/\omega} \approx \frac{1}{2\pi/\omega}\int_0^{2\pi/\omega} \sin^2\omega t dt \tag{4.10.28}$$

$$\approx \frac{1}{2\pi/\omega}\int_0^{2\pi/\omega} \cos^2\omega t dt \tag{4.10.29}$$

$$\approx \frac{1}{2} \tag{4.10.30}$$

Since in oscillatory flow there is no net flow forward, this pumping power is "wasted" in the sense that it is not being utilized to a useful end. Thus in pulsatile flow, at low frequency, the total power required to drive the flow is equal to the power required to drive the steady part of the flow, as in Poiseuille flow, plus one half of that amount to maintain the oscillation of the oscillatory part of the flow. Pumping power with $\Omega = 1.0$ is shown in Fig.4.10.4.

4.11 Oscillatory Flow at High Frequency

At high frequency oscillatory flow in a tube is less able to keep pace with the changing pressure, thus reaching less than the fully developed Poiseuille flow profile at the peak of each cycle. The higher the frequency, the lower the peak velocity the flow is able to reach. In the limit of infinite frequency the velocity reached at the peak of each cycle is zero, that is, the fluid does not move at all. An interesting question is whether the pumping power required to maintain this limiting state of zero flow is zero. In this section we develop approximate expressions describing properties of oscillatory flow at high frequency, which are easier to use than the more general expressions involving Bessel functions and which will be used to answer this question.

An approximate expression for $J_0(\zeta)$ when ζ is large is given by [4,5]

$$J_0(\zeta) \approx \frac{\sin\zeta + \cos\zeta}{\sqrt{\pi\zeta}} \tag{4.11.1}$$

For the purpose of algebraic manipulation we write $\zeta = i\zeta_1$ so that

$$J_0(\zeta) \approx \frac{\sin(i\zeta_1) + \cos(i\zeta_1)}{\sqrt{\pi i\zeta_1}}$$

$$\approx \frac{i\sinh\zeta_1 + \cosh\zeta_1}{\sqrt{\pi i\zeta_1}}$$

$$\approx \frac{(1+i)}{2}\frac{e^{\zeta_1}}{\sqrt{\pi i\zeta_1}} \tag{4.11.2}$$

and similarly, writing $\Lambda = i\Lambda_1$,

$$J_0(\Lambda) \approx \frac{(1+i)}{2}\frac{e^{\Lambda_1}}{\sqrt{\pi i\Lambda_1}} \tag{4.11.3}$$

Near the tube wall where $r/a \approx 1$: Inserting the above approximations into Eq.4.6.2 for the velocity profile, and recalling from Eq.4.5.4 that $\zeta = \Lambda r/a$, hence $\zeta_1 = \Lambda_1 r/a$, we find

$$\frac{u_\phi(r,t)}{\hat{u}_s} = \frac{-4}{\Lambda^2}\left(1 - \frac{J_0(\zeta)}{J_0(\Lambda)}\right)e^{i\omega t}$$

$$\approx \frac{-4}{\Lambda^2}\left(1 - \sqrt{\frac{\Lambda_1}{\zeta_1}}e^{(\zeta_1-\Lambda_1)}\right)e^{i\omega t}$$

$$\approx \frac{-4}{\Lambda^2}\left(1 - \sqrt{\frac{a}{r}}e^{\Lambda_1(\frac{r}{a}-1)}\right)e^{i\omega t}$$

$$\approx \frac{4i}{\Lambda}\left(1 - \frac{r}{a}\right)e^{i\omega t} \tag{4.11.4}$$

The real and imaginary parts of which are given by

$$\frac{u_{\phi R}(r,t)}{\hat{u}_s} \approx \frac{2\sqrt{2}}{\Omega}\left(1 - \frac{r}{a}\right)(\cos\omega t + \sin\omega t) \tag{4.11.5}$$

$$\frac{u_{\phi I}(r,t)}{\hat{u}_s} \approx \frac{2\sqrt{2}}{\Omega}\left(1 - \frac{r}{a}\right)(\sin\omega t - \cos\omega t) \tag{4.11.6}$$

Near the center of the tube, where $r/a \approx 0$ but Λ is large because of high frequency: Here the ratio $J_0(\zeta)/J_0(\Lambda)$ in the expression for the velocity (Eq.4.6.2) requires an approximation of $J_0(\zeta)$ for *small* ζ and an expansion of $J_0(\Lambda)$ for *large* Λ. The ratio ultimately vanishes, with the result

$$\frac{u_\phi(r,t)}{\hat{u}_s} = \frac{-4}{\Lambda^2}e^{i\omega t} \tag{4.11.7}$$

the real and imaginary parts of which are given by

$$\frac{u_{\phi R}(r,t)}{\hat{u}_s} \approx \frac{4}{\Omega^2}\sin\omega t \tag{4.11.8}$$

$$\frac{u_{\phi I}(r,t)}{\hat{u}_s} \approx \frac{-4}{\Omega^2}\cos\omega t \tag{4.11.9}$$

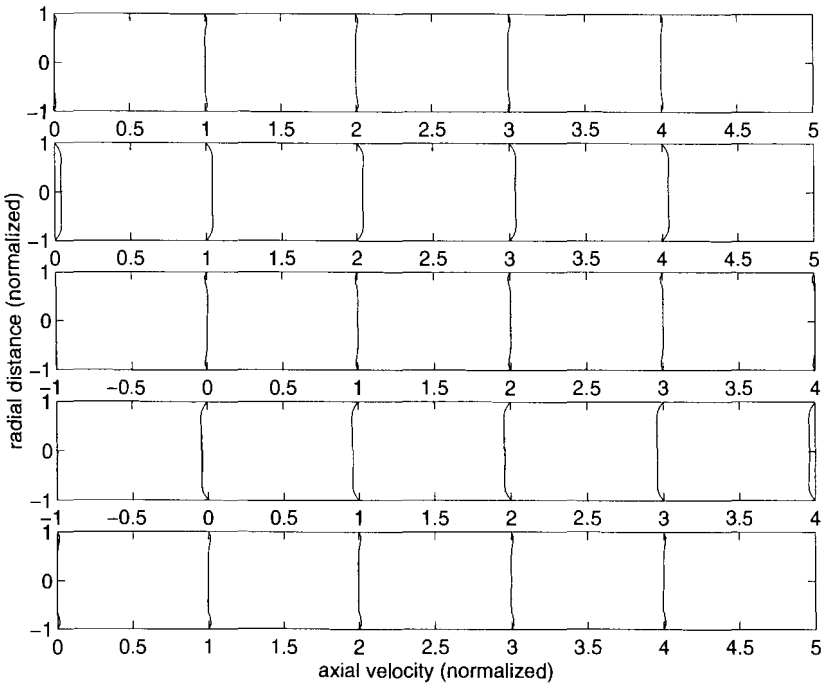

FIGURE 4.11.1. Oscillatory velocity profiles in a rigid tube at high frequency ($\Omega = 10$) and corresponding to the *real* part of the pressure gradient, namely, $k_s \cos\omega t$. The panels represent the profiles at different phase angles (ωt) within the oscillatory cycle, with $\omega t = 0$ in the top panel then increasing by 90° for subsequent panels. While the velocity is everywhere near zero, the profiles reach their peak form in the second panel, which means that they are about 90° out of phase with the pressure gradient (see text).

These results indicate that at high frequency fluid near the tube wall is affected differently from fluid near the center of the tube, thus distorting the parabolic character of the velocity profile. There is some phase difference between the velocity near the center of the tube and that near the wall. By contrast, at *low* frequency fluid is affected more uniformly by pulsation, and the parabolic character of the velocity profile is fairly well preserved during the oscillatory cycle, as we saw in the previous section. Velocity profiles with $\Omega = 10$ are shown in Fig.4.11.1.

For the flow rate, similarly, we use the approximation for large ζ of the Bessel function of first order, namely [4,5],

$$J_1(\zeta) \approx \frac{\sin\zeta - \cos\zeta}{\sqrt{\pi\zeta}} \tag{4.11.10}$$

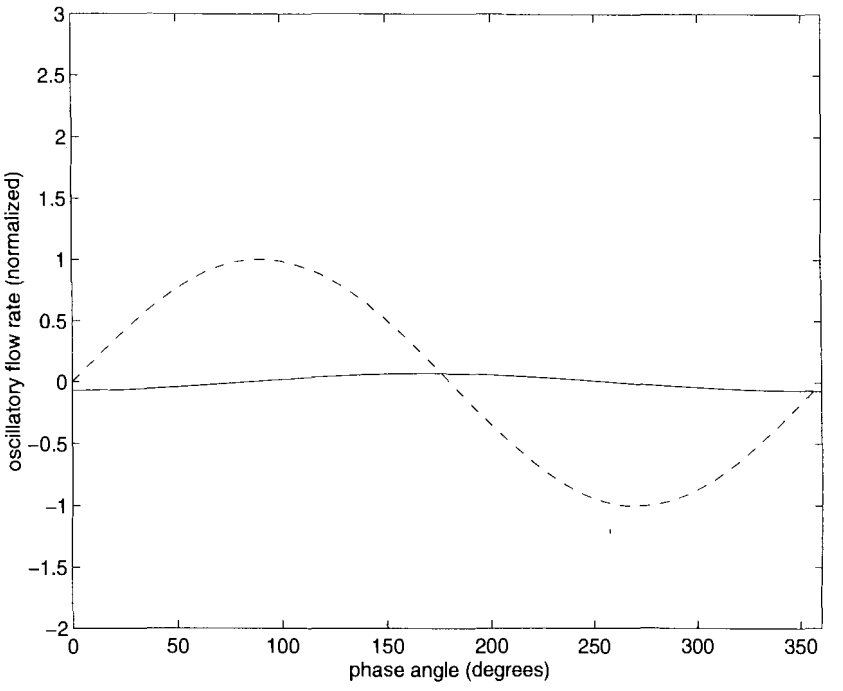

FIGURE 4.11.2. Variation of the oscillatory flow rate q_ϕ within an oscillatory cycle (solid line), compared with variation of the corresponding pressure gradient, in this case $k_{\phi I} = k_s \sin\omega t$ (dashed line), at high frequency ($\Omega = 10$). Flow rate is almost zero throughout the cycle, but there is an approximately 90° phase difference between flow rate and pressure gradient.

As before, writing $\zeta = i\zeta_1$, $\Lambda = i\Lambda_1$, gives

$$J_1(\zeta) \approx \frac{(i-1)e^{\zeta_1}}{2\sqrt{\pi i\zeta_1}} \tag{4.11.11}$$

$$J_1(\Lambda) \approx \frac{(i-1)e^{\Lambda_1}}{2\sqrt{\pi i\Lambda_1}} \tag{4.11.12}$$

and substituting into Eq.4.7.7 we get

$$\begin{aligned} \frac{q_\phi(t)}{q_s} &= \frac{-8i}{\Omega^2}\left(1 - \frac{2J_1(\Lambda)}{\Lambda J_0(\Lambda)}\right)e^{i\omega t} \\ &\approx \frac{-8i}{\Omega^2}\left(1 - \frac{2}{i\Omega^2}\frac{(i-1)}{(i+1)}\right)e^{i\omega t} \\ &\approx \frac{8}{\Omega^2}\left(\sin\omega t - i\cos\omega t\right) \end{aligned} \tag{4.11.13}$$

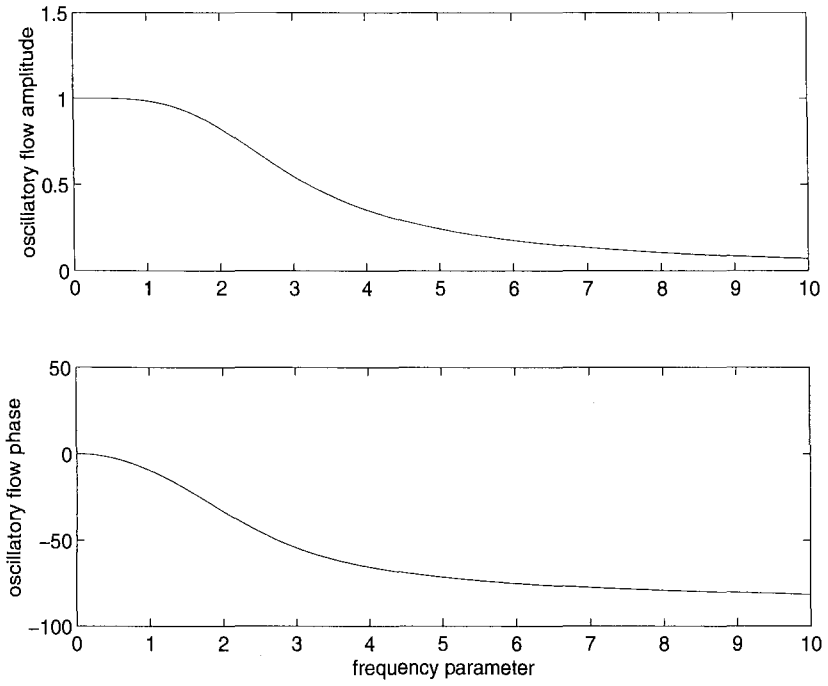

FIGURE 4.11.3. Variation of amplitude and phase of the oscillatory flow rate q_ϕ with frequency parameter Ω. The amplitude (normalized in terms of corresponding steady flow rate) is near 1.0 at low frequency but drops rapidly to near zero as the frequency increases. The phase angle (representing the phase difference between flow rate and pressure gradient, in degrees) is near zero at low frequency but drops rapidly to $-90°$ as the frequency increases.

where the term containing $1/\Omega^2$ is neglected in the last step, and recalling that $\Lambda^2 = -i\Omega^2$. The real and imaginary parts are given by

$$\frac{q_{\phi R}(t)}{q_s} \approx \left(\frac{8}{\Omega^2}\right) \sin \omega t \tag{4.11.14}$$

$$\frac{q_{\phi I}(t)}{q_s} \approx \left(\frac{-8}{\Omega^2}\right) \cos \omega t \tag{4.11.15}$$

These results are similar to those for velocity near the center of the tube (Eq.4.11.8,9), thus flow rate behaves like velocity near the center of the tube, as expected. The results also show how flow rate diminishes at high frequency, as shown in Figs.4.11.2,3.

Corresponding results for shear stress, omitting the details, are given by

$$\frac{\tau_{\phi R}(r,t)}{\tau_s} \approx \left(\frac{\sqrt{2}}{\Omega}\right) (\sin \omega t + \cos \omega t) \tag{4.11.16}$$

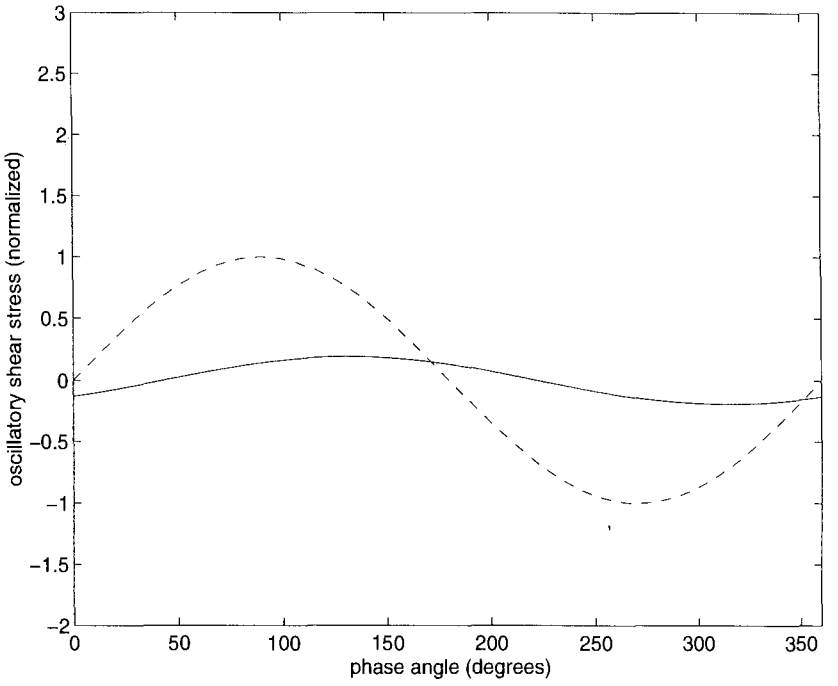

FIGURE 4.11.4. Variation of the imaginary part of oscillatory shear stress $\tau_{\phi I}$ (solid line) compared with the corresponding part of the pressure gradient $k_{\phi I}$ (dashed line), at high frequency ($\Omega = 10$). Shear stress is very low at high frequency, but there is an approximately 90° phase difference between shear stress and pressure gradient.

$$\frac{\tau_{\phi I}(r,t)}{\tau_s} \approx \left(\frac{\sqrt{2}}{\Omega}\right) (\sin \omega t - \cos \omega t) \tag{4.11.17}$$

Variation of shear stress within the oscillatory cycle, and with $\Omega = 10$, is shown in Fig.4.11.4.

For the pumping power, using Eqs.4.9.16,17 and results above for the flow rate, we find

$$\begin{aligned} \frac{H_{\phi I}}{H_s} &= \left(\frac{k_{\phi I}}{k_s}\right)\left(\frac{q_{\phi I}}{q_s}\right) \\ &\approx \frac{-8}{\Omega^2} \sin \omega t \cos \omega t \end{aligned} \tag{4.11.18}$$

$$\begin{aligned} \frac{H_{\phi R}}{H_s} &= \left(\frac{k_{\phi R}}{k_s}\right)\left(\frac{q_{\phi R}}{q_s}\right) \\ &\approx \frac{8}{\Omega^2} \cos \omega t \sin \omega t \end{aligned} \tag{4.11.19}$$

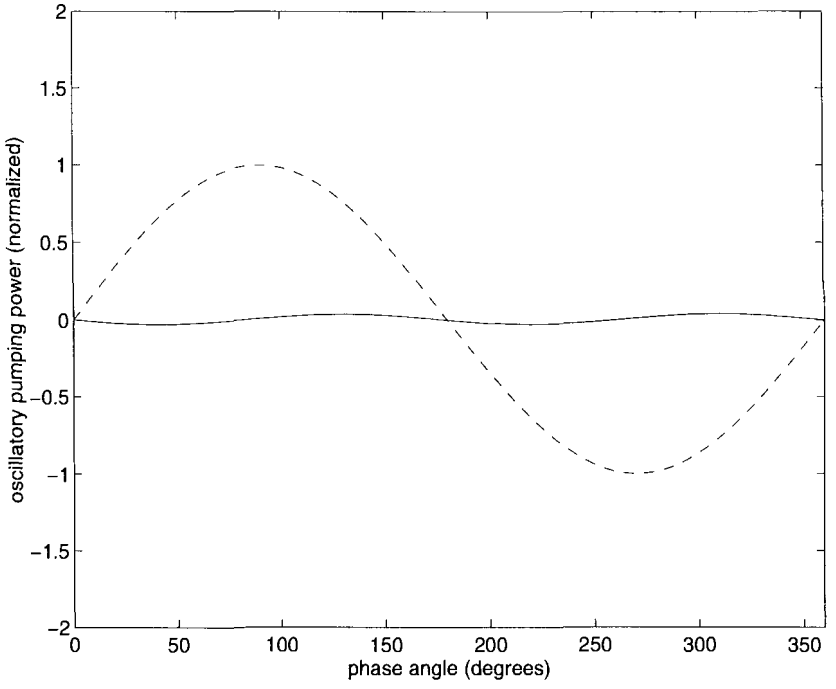

FIGURE 4.11.5. Variation of oscillatory pumping power $H_{\phi I}$ during one cycle (solid line) compared with the corresponding pressure gradient $k_{\phi I}$ (dashed line), at high frequency ($\Omega = 10$). Pumping power is near zero at high frequency, as expected because oscillatory flow rate and shear stress are near zero. By contrast, oscillatory pumping power at *low* frequency is one half the corresponding power in steady flow, even though the *net* flow forward is zero.

In both cases the pumping power vanishes in the limit of very high frequency. Note also, however, that at moderately high frequency where the above expressions can be used for calculating the power, the energy expenditure over one cycle based on these expressions is zero because of Eq.4.10.27. Variation of oscillatory pumping power within the oscillatory cycle, and with $\Omega = 10$, is shown in Fig.4.11.5.

4.12 Oscillatory Flow in Tubes of Elliptic Cross Sections

Pulsatile flow described in this chapter so far relates exclusively to flow in a tube of *circular* cross section. Flow in tubes of noncircular cross sections has not been studied as extensively as that in tubes of circular cross section, and there have been very few studies of *pulsatile* flow in such tubes [11–15]. The problem of pulsatile flow in tubes of *elliptic* cross sections is of particular interest because it offers the possibility of an exact analytical solution. Also, changing the ellipticity of an elliptic cross section produces a wide range of cross sections, including the circular cross section as a special case. Finally, a tube of elliptic cross section provides a good analytical model of a "compressed" blood vessel, which has considerable relevance in pulsatile blood flow.

Solution of the governing equation for pulsatile flow in a tube of elliptic cross section has been obtained in terms of Mathieu functions [11,15,17]. These functions are not as easy to evaluate as Bessel functions, which makes the solution not as readily usable as that for a tube of circular cross section. A brief outline of this solution is presented in this section, with some possible simplifications that make the solution more easy to use, and some results to highlight the effects of ellipticity on pulsatile flow in a tube.

The equation governing the flow is the same as that for a tube of circular cross section, namely, Eq.4.2.7. Boundary conditions are the same as those used for steady flow in a tube of elliptic cross section, namely Eq.3.10.2.

Because the boundary condition is being prescribed on the elliptic boundary of the cross section, solution of Eq.4.2.7 for pulsatile flow seems only possible by transforming to elliptic coordinates [16]

$$\begin{aligned} y &= d\cosh\xi\cos\eta \\ z &= d\sinh\xi\sin\eta \end{aligned} \tag{4.12.1}$$

where y, z are rectangular coordinates in the plane of the elliptic cross section and $2d$ is the distance between the two foci of the ellipse. The curves of constant η represent a family of confocal hyperbolas, while the curves of constant ξ represent a family of confocal ellipses, as illustrated in Fig.4.12.1. The coordinate ξ varies from 0 on the interfocal line to ξ_o on the tube wall. In terms of the elliptic coordinates ξ, η, the governing equation (Eq.4.2.7) with no-slip at the tube wall becomes

$$\frac{2\mu}{d^2(\cosh 2\xi - \cos 2\eta)}\left(\frac{\partial^2 u_{\phi e}}{\partial \xi^2} + \frac{\partial^2 u_{\phi e}}{\partial \eta^2}\right) - \rho\frac{\partial u_{\phi e}}{\partial t} = k_{\phi e}(t) \tag{4.12.2}$$

$$u_{\phi e}(\xi_o, \eta) = 0 \tag{4.12.3}$$

where subscript ϕ is being used as in Section 4.2 to denote oscillatory flow, subscript e is being added as in Section 3.10 to denote elliptic cross section, and $k_{\phi e}$ is the oscillatory pressure gradient in the elliptic tube.

Solution is obtained for an oscillatory pressure gradient as in the case of oscillatory flow in a tube of circular cross section (Eq.4.4.1), that is,

$$k_{\phi e} = k_s e^{i\omega t} \tag{4.12.4}$$

the amplitude k_s being taken the same as that in steady flow in tubes of circular and elliptic cross sections, to facilitate comparison.

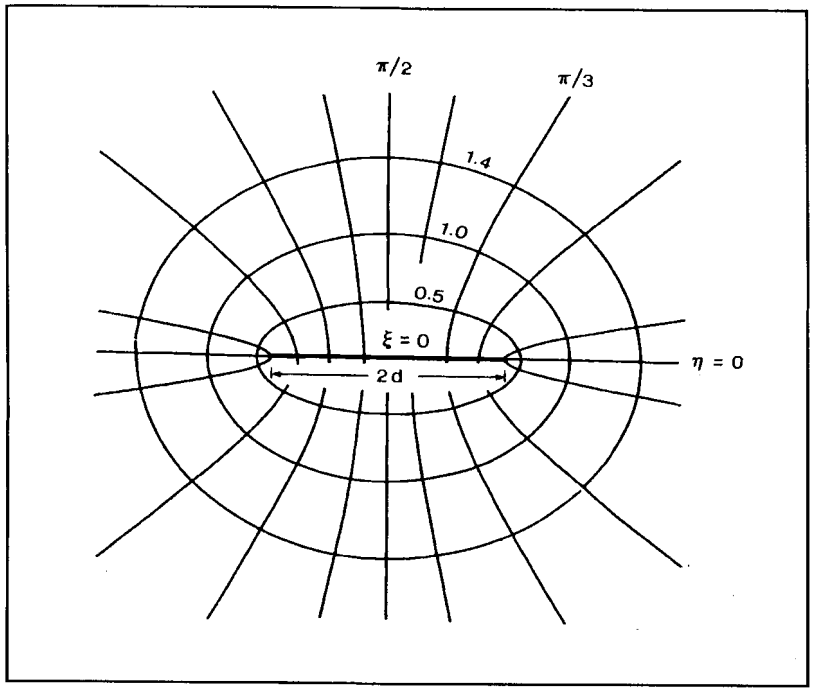

FIGURE 4.12.1. Elliptic coordinate system used in the solution and description of flow in tubes of elliptic cross sections. From [15].

With this choice of pressure gradient the oscillatory part of the velocity takes the form

$$u_{\phi e}(\xi,\eta,t) = U_{\phi e}(\xi,\eta)e^{i\omega t} \tag{4.12.5}$$

and the governing equation finally becomes an equation for $U_{\phi e}$, namely,

$$\frac{2}{d^2(\cosh 2\xi - \cos 2\eta)}\left(\frac{\partial^2 U_{\phi e}}{\partial \xi^2} + \frac{\partial^2 U_{\phi e}}{\partial \eta^2}\right) - \frac{i\rho\omega}{\mu}U_{\phi e} = \frac{k_s}{\mu} \tag{4.12.6}$$

A nondimensional frequency parameter is defined by

$$\Omega_e = \sqrt{\frac{\rho\omega}{\mu}}\sigma \tag{4.12.7}$$

where

$$\sigma = \sqrt{\frac{2b^2c^2}{b^2+c^2}} \tag{4.12.8}$$

and b, c are semi-minor and semi-major axes of the ellipse as in the steady-flow case.

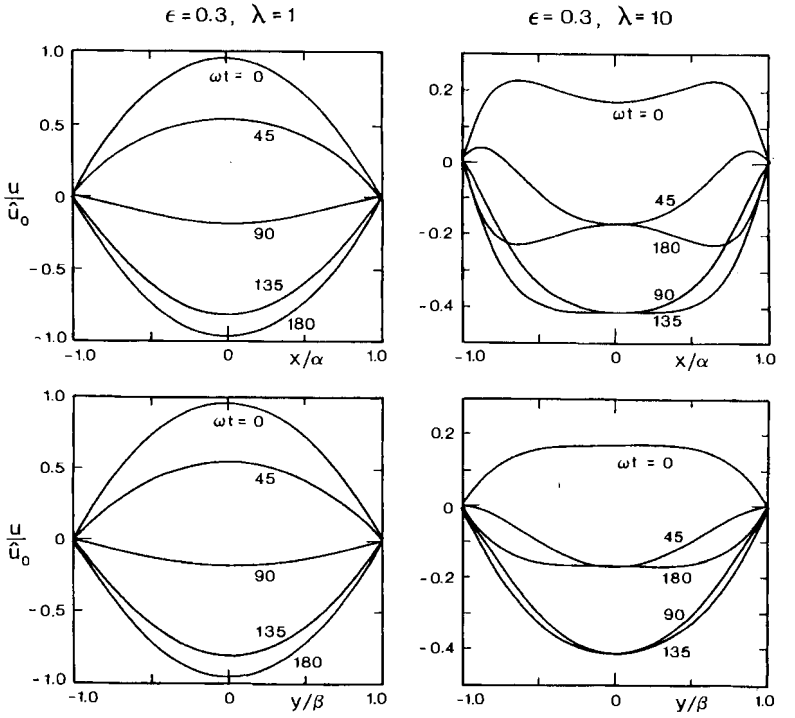

FIGURE 4.12.2. Oscillatory velocity profiles along the major axis (top) and minor axis (bottom) of an elliptic cross section at low ($\lambda = 1$, left) and moderately high frequency ($\lambda = 10$, right). In each panel, velocity profiles are shown at different phase angles ωt within the oscillatory cycle, ranging from $\omega t = 0°$ to $\omega t = 180°$, the second half of the cycle being omitted because of symmetry. The coordinates x, y and the axes α, β in this figure, from [15], correspond to coordinates y, z and axes b, c used in this book. The parameter λ corresponds to the square of the frequency parameter Ω_e used in this book. The effects of ellipticity on the flow are here seen in terms of the difference between velocity profiles along the major axis in the top panels and minor axis in the bottom panels. The difference is seen to be insignificant at low frequency, but becomes considerable at high frequency.

Equation 4.12.6 has a solution of the form [15]

$$U_{\phi e}(\xi,\eta) = \frac{4\hat{u}_{se}}{i\Omega^2} + \sum_{n=0}^{\infty} C_{2n} Ce_{2n}(\xi,-\gamma)\, ce_{2n}(\eta,-\gamma) \tag{4.12.9}$$

where C_{2n} is a constant determined by the boundary condition, ce_{2n} and Ce_{2n} are the ordinary and modified Mathieu functions [17], and

$$\gamma = \frac{i\rho\omega d^2}{4\mu} \tag{4.12.10}$$

Some velocity profiles are shown in Fig.4.12.2 and oscillatory flow rate in Fig.4.12.3.

Evaluation of this solution is highly cumbersome because of the infinite series in Eq.4.12.9 and because of the difficulties involved in the evaluation of Mathieu functions in general. Some simplifications are possible, however, under certain conditions.

At *low frequency* it is found that velocity and flow rate can be put in the form

$$u_{\phi e}(y,z,t) \approx u_{se}(y,z)e^{i\omega t} \tag{4.12.11}$$

$$q_{\phi e}(t) \approx q_{se}e^{i\omega t} \tag{4.12.12}$$

where u_{se} and q_{se} are the corresponding velocity and flow rate in *steady* flow in a tube of elliptic cross section (Eqs.3.10.3,4).

At *low ellipticity* ($\epsilon = b/c$) it is found that velocity and flow rate become very close to those in a tube of circular cross section, with the radius of the tube being replaced by σ. In fact, for $\epsilon > 0.9$ it is found that differences from the circular case are negligibly small.

Finally, it has been found that the ratio $q_{\phi e}/q_{se}$ at *all frequencies* is highly insensitive to the value of ellipticity ϵ. In particular, therefore, this ratio for a tube of elliptic cross section is approximately equal to the corresponding ratio for a tube of circular cross section, that is,

$$\frac{q_{\phi e}(t)}{q_{se}} \approx \frac{q_{\phi}(t)}{q_s} \tag{4.12.13}$$

the flow rates on the right-hand side being those for a tube of circular cross section (Eqs.3.4.3, 4.7.5). This permits the following approximation for the flow rate in a tube of elliptic cross section, using Eq.4.7.5

$$\frac{q_{\phi e}(t)}{q_{se}} \approx \frac{-8}{\Lambda_e^2}\left(1 - \frac{2J_1(\Lambda_e)}{\Lambda_e J_0(\Lambda_e)}\right)e^{i\omega_e t} \tag{4.12.14}$$

where

$$\Lambda_e = \left(\frac{i-1}{\sqrt{2}}\right)\Omega_e \tag{4.12.15}$$

and Ω_e, which contains the parameter σ replacing the radius of the circular cross section, is defined by Eq.4.12.7. This approximate expression for the flow rate is clearly much easier to use than one derived from Eq.4.12.9, and the approximation is equally valid for the full range of frequency and ellipticity.

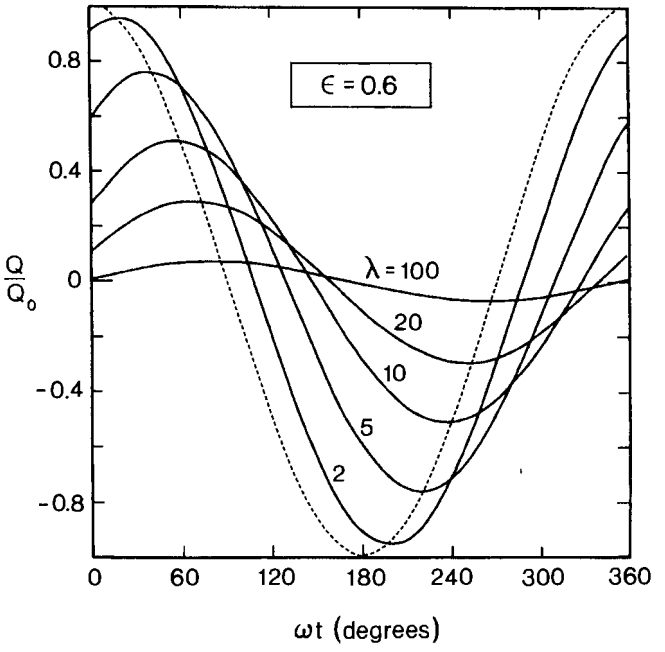

FIGURE 4.12.3. Oscillatory flow rate in a tube of elliptic cross section of ellipticity $\epsilon = 0.6$, normalized in terms of the corresponding steady-flow rate. The ratio Q/Q_0 and parameter λ in this figure, from [15], correspond to the ratio $q_{\phi e}/q_{se}$ and the square of the frequency parameter Ω_e used in this book. Each curve represents variation of the flow rate within one oscillatory cycle for a given value of the frequency parameter. The dotted curve represents the corresponding pressure gradient. As in the case of a tube of circular cross section, flow rate is in phase with pressure gradient at low frequency, but becomes increasingly out of phase and diminishes in magnitude as the frequency increases.

4.13 Problems

1. Explain a principal feature of oscillatory flow in a rigid tube that makes it somewhat artificial physiologically.
2. State the main assumption that makes it possible to separate the equations governing the steady and oscillatory parts of pulsatile flow in a rigid tube, as in Eq.4.2.2, and explain the restrictions that this places on the flow being considered.
3. Instead of two separate sine and cosine series, the harmonics of a composite oscillatory wave can always be put in the form of only a cosine series in which each term has an amplitude C and a phase angle Φ, that

is, in the notation of Eq.4.3.2

$$f(t) = \sum_{n=1}^{\infty} C_n \cos\left(\frac{2n\pi t}{T} + \Phi_n\right)$$

The first 10 harmonics of the composite wave shown in Fig.4.3.1 have the following amplitudes and phase angles (in degrees)

7.5803	-173.9168
5.4124	88.9222
1.5210	-21.7046
0.5217	-33.5372
0.8311	-126.8094
0.6851	135.0559
0.2584	152.0862
0.5408	44.0552
0.2715	-72.0738
0.0991	11.3354

Write down the expressions required to compute the first four harmonics shown in Fig.4.3.2, and indicate the way in which approximations for the composite wave shown in Fig.4.3.1 would be constructed from these.

4. Show by substitution that separation of variables in Eq.4.4.3 reduces the *partial* differential equation (Eq.4.4.2) into the *ordinary* differential equation (Eq.4.4.4).

5. The first term on the right-hand side in Eq.4.5.1 for the solution of Bessel equation represents a *particular* solution of Eq.4.4.4. Show by substitution that

$$U_\phi(r) = \frac{ik_s a^2}{\mu\Omega^2}$$

does satisfy that equation.

6. The second and third terms on the right-hand side in Eq.4.5.1 for the solution of Bessel equation represent two independent solutions of the *homogeneous* form of Eq.4.4.4. Show by substitution that each of

$$U_\phi(r) = AJ_0(\zeta), \quad U_\phi(r) = BY_0(\zeta)$$

satisfies the homogeneous form of Eq.4.4.4.

7. Consider pulsatile flow in a rigid tube with frequency $\Omega = 3.0$ and driving pressure gradient of the form $k_s \cos\omega t$. Using Eq.4.6.2 and values of Bessel functions in Appendix A, find the velocity at the center of the tube (a) at the beginning of the cycle and (b) at a quarter way through the cycle. Compare your results with those in Fig.4.6.1.

8. Consider pulsatile flow in a rigid tube with frequency $\Omega = 3.0$ and driving pressure gradient of the form $k_s \sin\omega t$. Using Eq.4.7.7 and values of Bessel functions in Appendix A, find the peak flow rate, which, according to Fig.4.7.1, occurs at $\omega t \approx 150°$. Compare your result with that in Fig.4.7.1.

9. Results in Fig.4.9.1 indicate that in oscillatory flow the average rate of energy dissipation at the tube wall is nonzero, therefore requiring pumping power to maintain. In *pulsatile* flow, consisting of oscillatory plus steady flow components, this "wasted" pumping power would be required in addition to that required for the steady part of the flow. Use Eqs.4.9.16,17 to calculate the average of this wasted power over one oscillatory cycle, expressed as a fraction of the corresponding pumping power in steady flow. Use $\Omega = 3.0$ in the calculation, then compare the result with that in Fig.4.9.1

10. Use approximate expressions for low and for high frequency to compare the peak flow rates reached at $\Omega = 1$ and $\Omega = 10$, and compare the results visually with those in Fig.4.11.3.

11. From the results of the previous example, deduce the phase lag of flow behind pressure gradient at low ($\Omega = 1$) and high ($\Omega = 10$) frequency. Compare the results visually with those in Fig.4.11.3.

12. The back and forth movements of the fluid in oscillatory flow waste energy not because of acceleration and deceleration of the fluid but because of viscous dissipation at the tube wall. Use the results of Sections 4.10 and 4.11 to determine if this wasteful energy expenditure is higher at high or low frequency, and determine its magnitude at $\Omega = 1$ and $\Omega = 10$, expressed as a fraction of the corresponding pumping power in steady flow.

4.14 References and Further Reading

1. Lighthill M, 1975. Mathematical Biofluiddynamics. Society for Industrial and Applied Mathematics, Philadelphia.
2. Walker JS, 1988. Fourier Analysis. Oxford University Press, New York.
3. Brigham EO, 1988. The Fast Fourier Transform and its Applications. Prentice Hall, Englewood Cliffs, New Jersey.
4. McLachlan NW, 1955. Bessel Functions for Engineers. Clarendon Press, Oxford.
5. Watson GN, 1958. A Treatise on the Theory of Bessel Functions. Cambridge University Press. Cambridge.
6. Sexl T, 1930. Über den von E.G. Richardson entdeckten "Annulareffekt." Zeitschrift für Physik 61:349–362.
7. Womersley JR, 1955. Oscillatory motion of a viscous liquid in a thin-walled elastic tube—I: The linear approximation for long waves. Philosophical Magazine 46:199–221.
8. Uchida S, 1956. The pulsating viscous flow superimposed on the steady laminar motion of incompressible fluid in a circular pipe. Zeitschrift für angewandte Mathematik und Physik 7:403-422.

9. McDonald DA, 1974. Blood flow in arteries. Edward Arnold, London.
10. Milnor WR, 1989. Hemodynamics. Williams and Wilkins, Baltimore.
11. Khamrui SR, 1957. On the flow of a viscous liquid through a tube of elliptic section under the influence of a periodic gradient. Bulletin of the Calcutta Mathematical Society 49:57–60.
12. Begum R, Zamir M, 1990. Flow in tubes of non-circular cross sections. In: Rahman M (ed), Ocean Waves Mechanics: Computational Fluid Dynamics and Mathematical Modeling. Computational Mechanics Publications, Southampton.
13. Duan B, Zamir M, 1991. Approximate solution for pulsatile flow in tubes of slightly noncircular cross-sections. Utilitas Mathematica 40:13–26.
14. Quadir R, Zamir M, 1997. Entry length and flow development in tubes of rectangular and elliptic cross sections. In: Rahman M (ed), Laminar and Turbulent Boundary Layers. Computational Mechanics Publications, Southampton.
15. Haslam M, Zamir M, 1998. Pulsatile flow in tubes of elliptic cross sections. Annals of Biomedical Engineering 26:1–8.
16. Moon PH, Spencer DE, 1961. Field Theory for Engineers. Van Nostrand, Princeton, New Jersey.
17. McLachlan NW, 1964. Theory and Application of Mathieu Functions. Dover Publications, New York.

5

Pulsatile Flow in an Elastic Tube

5.1 Introduction

In the case of a *rigid* tube it is possible to postulate a fully developed region away from the tube entrance where the flow is independent of x, thus derivatives of u, v with respect to x are zero. The equation of continuity combined with the boundary condition $v=0$ at the tube wall then leads to v being identically zero and the governing equations reduce to (Eq.3.2.9)

$$\rho\frac{\partial u}{\partial t}+\frac{\partial p}{\partial x}=\mu\left(\frac{\partial^2 u}{\partial r^2}+\frac{1}{r}\frac{\partial u}{\partial r}\right)$$

As we saw in Chapter 4, the pressure gradient term in that case is a function of t only, not of x, and the velocity u is then a function of r, t only, not of x. For an oscillatory pressure gradient the velocity u then oscillates with the same frequency, and since it is not a function of x, it will represent the velocity at every cross section of the tube. The fluid then oscillates *in bulk*, or "en mass." *There is no wave motion* when the tube is rigid.

When the tube is *nonrigid*, because of movement of the tube wall the radial velocity v of the fluid can no longer be identically zero, and both u and v can no longer be independent of x even away from the tube entrance (Fig.5.1.1). Equation 3.2.9 is then no longer valid and we must return to the full Navier–Stokes equations, assuming only axial symmetry, that is (Eqs.3.2.2–4)

$$\rho\left(\frac{\partial u}{\partial t}+u\frac{\partial u}{\partial x}+v\frac{\partial u}{\partial r}\right) \quad + \quad \frac{\partial p}{\partial x}$$